

2-Amino-9H-pyrido[2,3-b]indole (AαC) Adducts and Thiol Oxidation of Serum Albumin as Potential Biomarkers of Tobacco Smoke*[§]

Received for publication, February 19, 2015, and in revised form, May 5, 2015. Published, JBC Papers in Press, May 7, 2015, DOI 10.1074/jbc.M115.646539

Khyatiben V. Pathak[‡], Medjda Bellamri[§], Yi Wang[‡], Sophie Langouët[§], and Robert J. Turesky[‡]^{¶1}

From the [‡]Masonic Cancer Center and Department of Medicinal Chemistry, University of Minnesota, Minneapolis, Minnesota 55455 and [§]UMR INSERM 1085 IRSET, Rennes 1 University, UMS 3480 Biosit, F-35043 Rennes, France

Background: The reactivity of AαC, a tobacco smoke carcinogen, was investigated with DNA and albumin of human hepatocytes.

Results: Hepatocytes bioactivate AαC to metabolites, which adduct to DNA and albumin.

Conclusion: Cys³⁴ and Met³²⁹ of serum albumin are targets for AαC electrophiles.

Significance: AαC forms macromolecular adducts and induces oxidative stress, which may be contributing factors to liver damage and cancer risk in smokers.

2-Amino-9H-pyrido[2,3-b]indole (AαC) is a carcinogenic heterocyclic aromatic amine formed during the combustion of tobacco. AαC undergoes bioactivation to form electrophilic *N*-oxidized metabolites that react with DNA to form adducts, which can lead to mutations. Many genotoxicants and toxic electrophiles react with human serum albumin (albumin); however, the chemistry of reactivity of AαC with proteins has not been studied. The genotoxic metabolites, 2-hydroxyamino-9H-pyrido[2,3-b]indole (HONH-AαC), 2-nitroso-9H-pyrido[2,3-b]indole (NO-AαC), *N*-acetyloxy-2-amino-9H-pyrido[2,3-b]indole (*N*-acetoxy-AαC), and their [¹³C₆]AαC-labeled homologues were reacted with albumin. Sites of adduction of AαC to albumin were identified by data-dependent scanning and targeted bottom-up proteomics approaches employing ion trap and Orbitrap MS. AαC-albumin adducts were formed at Cys³⁴, Tyr¹⁴⁰, and Tyr¹⁵⁰ residues when albumin was reacted with HONH-AαC or NO-AαC. Sulfenamide, sulfinamide, and sulfonamide adduct formation occurred at Cys³⁴ (AαC-Cys³⁴). *N*-Acetoxy-AαC also formed an adduct at Tyr³³². Albumin-AαC adducts were characterized in human plasma treated with *N*-oxidized metabolites of AαC and human hepatocytes exposed to AαC. High levels of *N*-(deoxyguanosin-8-yl)-AαC (dG-C8-AαC) DNA adducts were formed in hepatocytes. The Cys³⁴ was the sole amino acid of albumin to form adducts with AαC. Albumin also served as an antioxidant and scavenged reactive oxygen species generated by metabolites of AαC in hepatocytes; there was a strong decrease in reduced Cys³⁴, whereas the levels of Cys³⁴ sulfenic acid (Cys-SO₂H), Cys³⁴-sulfonic acid (Cys-SO₃H), and Met³²⁹ sulfoxide were greatly increased. Cys³⁴ adduction products and Cys-SO₂H, Cys-SO₃H,

and Met³²⁹ sulfoxide may be potential biomarkers to assess exposure and oxidative stress associated with AαC and other arylamine toxicants present in tobacco smoke.

Tobacco smoke is a major risk factor not only for lung cancer but also for cancer of the liver, bladder, and gastrointestinal tract (1–4). The combustion of tobacco produces many genotoxicants, including polycyclic aromatic hydrocarbons, nitrosamines, aromatic amines, and heterocyclic aromatic amines (HAAs),² which are potential human carcinogens (5). AαC was originally discovered as a mutagenic pyrolysis product of protein (6) and subsequently identified in cigarette smoke at levels ranging from 60 to 250 ng/cigarette (7, 8). These quantities are far greater than those of the aromatic amines 4-aminobiphenyl and 2-naphthylamine, which are implicated in the pathogenesis of bladder cancer in smokers (1, 9). Apart from the endocyclic nitrogen atoms, AαC shares the same structure as 2-aminofluorene, one of the most well studied aromatic amine carcinogens (10). Significant levels of AαC were detected in the urine of male smokers of the Shanghai cohort in China, providing evidence that tobacco smoke is a major source of AαC exposure (11). AαC is a liver carcinogen in mice, a transgene colon mutagen, and an inducer of colonic aberrant crypt foci, an early biomarker of colon neoplasia (12–14). Therefore, AαC could play a role in the incidence of liver or digestive tract cancers of smokers.

AαC undergoes metabolic activation by *N*-oxidation of the exocyclic amine group, by cytochrome P450 (P450) enzymes, to

* This work was supported, in whole or in part, by National Institutes of Health Grants RO1 CA134700 and RO1CA134700-03S1 of the Family Smoking Prevention and Tobacco Control Act. This work was also supported by PNREST Anses, Cancer TMOI AVIESAN (2013/1/166). The authors declare that they have no conflicts of interest with the contents of this article.

[§] This article contains supplemental Figs. S1–S4.

^{¶1} To whom correspondence should be addressed: Masonic Cancer Center and Dept. of Medicinal Chemistry, University of Minnesota, Minneapolis, MN 55455. Tel.: 612-626-0141; Fax: 612-624-3869; E-mail: rturesky@umn.edu.

² The abbreviations used are: HAA, heterocyclic aromatic amines; AαC, 2-amino-9H-pyrido[2,3-b]indole; *N*-acetoxy-AαC, *N*-acetyloxy-2-amino-9H-pyrido[2,3-b]indole; HONH-AαC, 2-hydroxyamino-9H-pyrido[2,3-b]indole; NO-AαC, 2-nitroso-9H-pyrido[2,3-b]indole; NO₂-AαC, 2-nitro-9H-pyrido[2,3-b]indole; P450, cytochrome P450; PhIP, 2-amino-1-methyl-6-phenylimidazo[4,5-b]pyridine; IAM, iodoacetamide; DDA, data-dependent acquisition; CID, collision-induced dissociation; HCD, high-energy collision dissociation; UPLC, ultraperformance liquid chromatography; ROS, reactive oxygen species; dG-C8-AαC, *N*-(deoxyguanosin-8-yl)-AαC; IAM, iodoacetamide; TIC, total ion chromatogram.

form 2-hydroxyamino-9H-pyrido[2,3-*b*]indole (HONH-A α C) (Fig. 1) (15, 16). HONH-A α C can undergo conjugation reactions with *N*-acetyltransferases or sulfotransferases to form unstable esters. These metabolites undergo heterolytic cleavage to form the proposed short lived nitrenium ion of A α C (Fig. 1) (17), which reacts with DNA to form covalent adducts, leading to mutations (18). The genotoxic potential of A α C has been shown in human peripheral blood lymphocytes (19), Chinese hamster ovary cells (18), and human hepatocytes (20), where high levels of A α C-DNA adducts are formed. However, long term stable biomarkers of A α C must be developed for implementation in molecular epidemiology studies that seek to address a role for this chemical in human cancer risk.

DNA adducts of A α C can be measured by sensitive liquid chromatography/mass spectrometry (LC/MS)-based methods (20). However, DNA from biopsy specimens is often unavailable, which restricts the use of this biomarker. The electrophilic *N*-oxidized metabolites of A α C are also expected to react with proteins (21). The biomonitoring of protein-carcinogen adducts is an alternative approach to assess exposure to hazardous chemicals. Stable carcinogen protein adducts do not undergo repair and are expected to follow the kinetics of the lifetime of the protein (22, 23). The major proteins in blood are hemoglobin (Hb) with a life span of 60 days, and human serum albumin with a half-life of 21 days. The chemistry of reactivity of Hb and albumin with various genotoxicants and toxic electrophiles has been reported (24–26), and several protein-carcinogen adducts have been employed to assess human exposures (23, 27, 28).

Our goal is to develop and implement protein-based biomarkers of A α C and other HAAs (29, 30) in molecular epidemiological studies designed to assess the role of HAAs in human cancers. In this study, we have examined the reactivity of albumin with *N*-oxidized metabolites of A α C. Cys³⁴ followed by Tyr¹⁴⁰ and Tyr¹⁵⁰ of albumin were major sites of adduction of A α C electrophiles. The Cys³⁴ and Met³²⁹ residues of albumin also served as scavengers of reactive oxygen species (ROS) generated by metabolites of A α C, and the Cys³⁴ sulfinic acid (Cys-SO₂H), sulfonic acid (Cys-SO₃H), and Met³²⁹ sulfoxide were recovered in high yield from human hepatocytes treated with A α C.

Experimental Procedures

Caution—A α C is a potential human carcinogen. A α C and its derivatives must be handled in a well ventilated fume hood with proper use of gloves and protective clothing.

Chemicals and Materials—A α C was purchased from Toronto Research Chemicals (Toronto, Canada). [4*b*,5,6,7,8,8*a*-¹³C₆]A α C was a gift from Dr. Daniel Doerge (National Center for Toxicological Research, Jefferson, AR). Albumin, trypsin, chymotrypsin, Pronase E, prolidase, leucine amino peptidase, β -mercaptoethanol, iodoacetamide (IAM), dithiothreitol (DTT), acetic anhydride, and palladium on carbon were obtained from Sigma-Aldrich. LC/MS grade solvents were from Fisher. Tetrahydrofuran was obtained from Alfa Aesar (Ward Hill, MA). Amicon ultracentrifugal filters (10 kDa cut-off) were purchased from Millipore (Billerica, MA). The Pierce albumin depletion kit was purchased from Thermo Scientific

(Rockford, IL). Human plasma was purchased from Bioreclamation LLC (Hicksville, NY).

Synthesis of *N*-Oxidized Metabolites of A α C—2-Nitro-9H-pyrido[2,3-*b*]indole (NO₂-A α C) and NO₂-[¹³C₆]A α C were prepared by oxidation of A α C with dimethyldioxirane (17). HONH-A α C and HONH-[¹³C₆]A α C were prepared by reduction of NO₂-A α C in tetrahydrofuran with hydrazine, using palladium on carbon as a catalyst (31). HONH-A α C was oxidized to 2-nitroso-9H-pyrido[2,3-*b*]indole (NO-A α C) with potassium ferricyanide (32). *N*-(Deoxyguanosin-8-yl)-A α C (dG-C8-A α C) and the isotopically labeled internal standards [¹³C₁₀]dG-C8-A α C were synthesized as described (33).

Modification of Albumin and Human Plasma with *N*-Oxidized Metabolites of A α C—Mixed disulfides formed at Cys³⁴ of commercial albumin (34) were reduced by treatment with β -mercaptoethanol (35). The reduced albumin was recovered in 100 mM potassium phosphate buffer (pH 7.4) employing Amicon Ultra centrifugal filters. The reduced albumin contained 0.98 mol of Cys³⁴/mol of albumin upon β -mercaptoethanol treatment. An equimolar solution of HONH-A α C and HNOH-[¹³C₆]A α C or *N*-acetoxy-A α C and *N*-acetoxy-[¹³C₆]A α C (15 nmol, in 10 μ l of EtOH) or NO-A α C (30 nmol in 10 μ l of EtOH) was reacted with albumin (0.6 nmol, 40 μ g) in 1 ml of 100 mM potassium phosphate buffer (pH 7.4) at 37 °C for 18 h. *N*-Acetoxy-A α C and *N*-acetoxy-[¹³C₆]A α C were prepared *in situ* by adding equimolar solution of HONH-A α C and HONH-[¹³C₆]A α C (15 nmol) to the solution of albumin, immediately followed by the addition of 450 nmol of acetic anhydride (36), and incubated at 37 °C for 1 h. The unreacted A α C metabolites were removed by ethyl acetate extraction. Human plasma (5 μ l, containing ~200 μ g of albumin, 3 nmol) was diluted with 1 ml of PBS and reacted with *N*-oxidized A α C derivatives as described above. Albumin from plasma was purified by affinity purification by Pierce albumin depletion kit. Other studies on A α C-albumin adduct formation were carried out using lower amounts of *N*-oxidized A α C (see below).

Human Hepatocyte Cell Culture—Human samples were obtained from the Centre de Ressources Biologiques (CRB)-Santé of Rennes. The research protocol was conducted under French legal guidelines and approved by the local institutional ethics committee. Hepatocytes were isolated by a two-step collagenase perfusion, and the parenchymal cells were seeded at a density of ~3 \times 10⁶ viable cells/19.5-cm² Petri dish in 3 ml of Williams' medium with supplements as reported (20), except fetal calf serum was replaced with human albumin (1 g/liter) pretreated with β -mercaptoethanol. After 2 days, the differentiated cells were incubated with A α C (20, 33).

Albumin and DNA Adduct Formation with A α C in Hepatocytes—Metabolism studies with A α C (0 or 50 μ M in DMSO, 0.01% (v/v)) were conducted for 24 h. A solution of 1:1 A α C and [¹³C₆]A α C (50 μ M) was employed for characterization of A α C-albumin adducts, whereas the DNA adduct studies employed A α C (50 μ M). The culture media containing albumin were removed after 24 h of incubation and immediately stored at -80 °C. The cells were washed with PBS, and cell pellets were collected by centrifugation at 3500 \times *g* for 10 min at 4 °C. Cells were stored at -80 °C until further use. Cell viability was determined by 3-(4,5-dimethylthiazol-2-yl)-2,5-diphenyltetrazolium

Characterization of A α C-Serum Albumin Adducts

bromide test, and treatment with A α C did not decrease cell viability (37). The medium was extracted with 3 volumes of ethyl acetate, and then the albumin was recovered with >85% purity by ethanol precipitation. For some analyses, the albumin (100 μ g, 1.5 nmol) was alkylated with a 100-fold molar excess of IAM (150 nmol) at 37 °C for 1 h. Excess IAM was removed by Amicon Ultra centrifugal filters.

Trypsin/Chymotrypsin Digestion—The digestion of A α C-modified albumin (10 μ g) was carried out using trypsin and chymotrypsin at a protease/protein ratio of 1:50 (w/w) and 1:25 (w/w), respectively, in 100 μ l of 50 mM ammonium bicarbonate buffer (pH 8.5) containing CaCl₂ (1 mM) at 37 °C for 16–18 h (35).

Pronase E/Leucine Aminopeptidase/Prolidase Digestion—Albumin (10 μ g, 150 pmol) was digested with Pronase E, leucine aminopeptidase, and prolidase at protease/protein ratios of 1:2 (w/w), 1:30 (w/w), and 1:8 (w/w), respectively, in 50 mM ammonium bicarbonate buffer (pH 8.5) containing MnCl₂ (1 mM) at 37 °C for 20 h (23). The A α C-amino acid adducts were enriched by solid phase extraction (32).

UPLC Mass Spectrometry Parameters for Peptide Analyses—Peptides were resolved with an Atlantis C18 nanoACQUITY column (0.3 mm \times 150 mm, 3- μ m particle size, 100 Å) (Waters Corp., Milford, MA) using solvent A (5% acetonitrile, 94.99% water, 0.01% formic acid) and solvent B (95% acetonitrile, 4.99% water, 0.01% formic acid) as mobile phases with a Thermo Dionex Ultimate 3000 Nano/Cap LC System connected to an Orbitrap Elite mass spectrometer (Thermo Scientific, San Jose, CA) using an Advance CaptiveSpray source (Auburn, CA) in the positive ionization mode.

A 60-min gradient (99% solvent A to 60% solvent B for 45 min, 60 to 99% solvent B at 45–60 min) and 25-min gradient (99% solvent A to 60% solvent B for 20 min and 60–90% solvent B for 20–25 min) at 5 μ l/min flow rate were used, respectively, for data-dependent (DDA) and targeted data acquisition.

The top five precursor ions for CID-MS/MS analysis with dynamic exclusion for 180 s with three repeats of 60-s repeat duration were selected for DDA. Mass tag DDA (MS tag DDA) was employed to trigger MS/MS on peptides and amino acid adducts displaying the characteristic pattern of a 1:1 isotopic mixture of A α C and [¹³C₆]A α C (38). The partner intensity ratio was 85–100%; m/z difference of 6 (singly charged), 3 (doubly charged), and 2 (triply charged) species. A mass list of precursor ions (Table 1) for A α C-amino acid and A α C-peptide adducts identified from MS tag DDA was used for targeted analysis.

The tune parameters were as follows: capillary tube temperature, 270 °C; spray voltage, 2.5 kV; S-lens RF level, 68(%); in-source fragmentation, 5 V; collision gas, helium; normalized collision energy, 35 eV; activation Q 0.3; HCD collision gas, argon; HCD collision energy, 20–35. Full scan data were acquired over a mass range of 150–1800 m/z at a resolving power of 120,000 (at 400 m/z), whereas MS/MS data acquisition was carried out with the ion trap or Orbitrap (resolving power 60,000) as mass analyzer with isolation widths 1.5 and 2 m/z . An internal lock mass at m/z 371.1012 (polysiloxane) was employed while using the Orbitrap mass analyzer. The tune parameters were optimized with LQQCPFEHVK and LQQCPF

peptides (New England Peptide, Gardner, MA). Mass spectral data were acquired with Xcalibur version 3.0.63 software.

Data Analysis of A α C-Albumin—The BumberDash platform (version 1.4.115) with the Myrimatch search algorithm (version 2.1.138) with a 31-protein subset of the RefSeq human protein database, version 37.3, with their forward and reverse protein sequences were used to search for the A α C-peptide adducts (29, 39). The dynamic modifications used in the Myrimatch configuration file were as follows: oxidation (+15.99 Da) on Met, Cys; deamidation (–17.03 Da) on N-terminal Gln; A α C and [¹³C₆]A α C (+181.06 and 187.11) on Cys, Lys, Tyr, Ser, Thr, Trp, His, Glu, Asp; SO-A α C and SO-[¹³C₆]A α C (+197.06, +203.10) on Cys and SO₂-A α C and SO₂-[¹³C₆]A α C (+213.05, +219.10); acetylation (+42.01) on Lys, Cys, Tyr, Arg. The search parameters used were as follows: enzyme (trypsin/chymotrypsin), up to two missed cleavages, mass tolerances 1.25 m/z (precursor ions) and 0.5 m/z (product ions). Each identified spectrum was filtered by the IDPicker algorithm (version 3.0.564) with a false discovery rate of 1%. The peptide sequences of identified A α C-peptide and A α C-amino acid adducts were confirmed by manually sequencing.

DNA Isolation and UPLC/MS³ Measurement of A α C-DNA Adducts—DNA was isolated by the phenol/chloroform method (20). DNA (5 μ g) was spiked with the isotopically labeled internal standard ([¹³C₁₀]dG-C8-A α C) at 1 adduct per 10⁶ bases, followed by enzymatic digestion of DNA (40). The UPLC/MS³ measurements of A α C-DNA adducts were performed using a NanoAcquity UPLC system (Waters Corp.) coupled with an LTQ VelosPro ion trap mass spectrometer (Fisher) as described previously (41). The ions were monitored with the MS³ scan mode. For dG-C8-A α C, ions at m/z 449.1 (MS) > 333.1 (MS²) > 209.2, 291.4, 316.4 (MS³) and for the internal standard, [¹³C₁₀]dG-C8-A α C, ions at m/z 459.1 (MS) > 338.1 (MS²) > 210.2, 295.4, 321.5 (MS³) were monitored (38).

Results

The metabolic activation of A α C in hepatocytes, the reaction of *N*-oxidized A α C metabolites with DNA and albumin, and the scavenging of ROS by albumin are summarized in Fig. 1.

The UV spectra of A α C, HONH-A α C, and NO-A α C are displayed in Fig. 2A. NO-A α C displays a red shift in its maximal absorbance compared with A α C and HONH-A α C. The product ion spectrum of A α C ([M + H]⁺ at m/z 184.1) displays fragment ions at m/z 167.0 and 157.1, attributed to the loss of NH₃ and HCN (Fig. 2B) (9). The product ion spectrum of NO-A α C ([M + H]⁺ at m/z 198.1) displays a sole ion at m/z 168.0 and is assigned to the loss of the NO group (Fig. 2C). The product ion spectrum of HONH-A α C ([M + H]⁺ at m/z 200.1) displays prominent fragment ions at m/z 182.1 and 183.1, which are attributed to the losses of H₂O and OH[•], and the product ion at m/z 155.1 is attributed to a loss of H₂O and HCN (Fig. 2D).

MS Tag DDA Mapping of A α C-Albumin Peptides and A α C-Amino Acid Adducts—The assignments of A α C-peptide adducts are based on CID and higher-energy collision dissociation (HCD) tandem MS.

The chromatograms of the MS tag DDA experiments of albumin modified with a 50-fold molar excess of *N*-oxidized A α C and [¹³C₆]A α C (1:1 ratio) were filtered using m/z values of

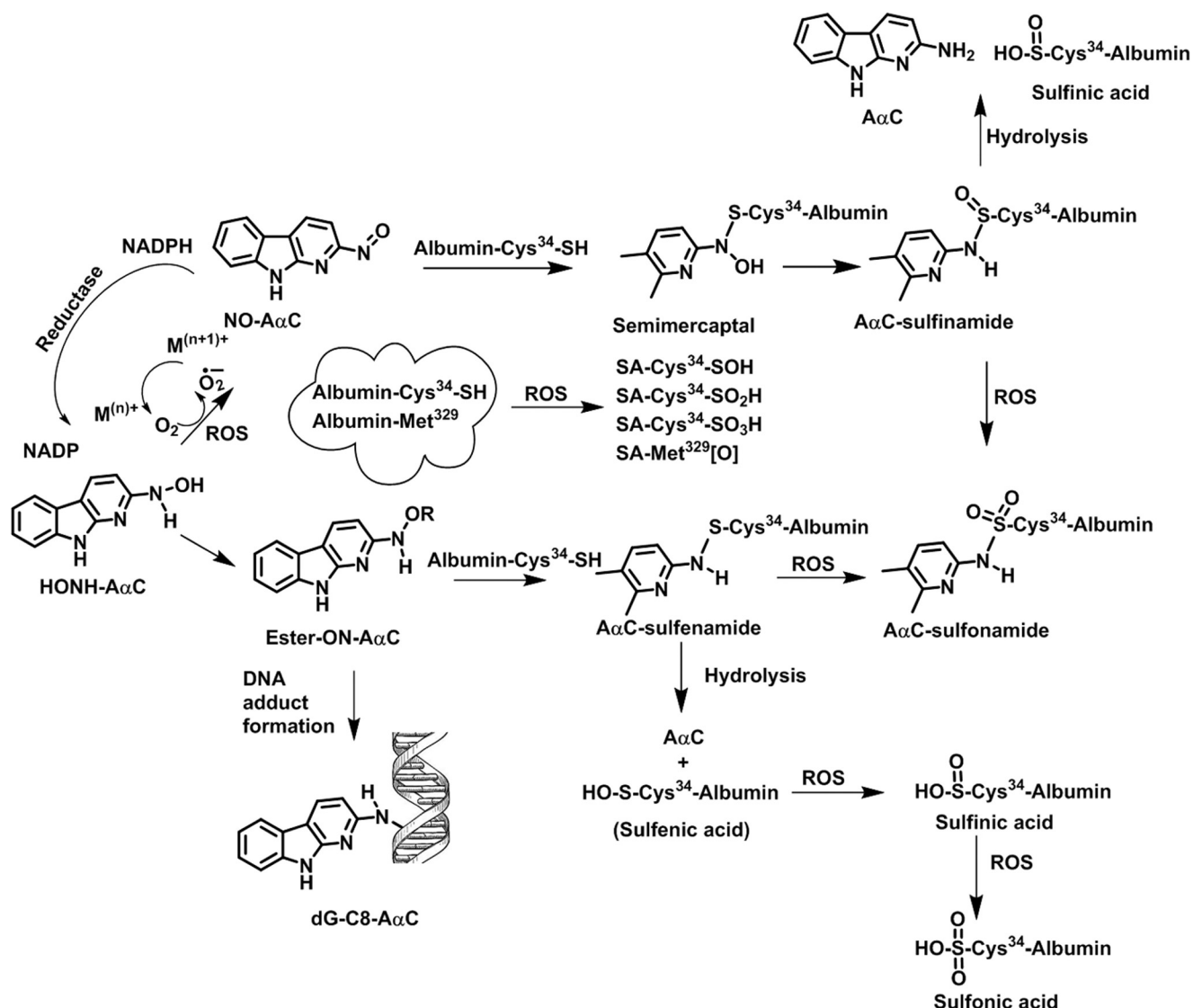


FIGURE 1. **Bioactivation of A α C, albumin adduct formation and induction of ROS in human hepatocytes.** A α C undergoes bioactivation by P450 to form HONH-A α C. The HONH-A α C and its *N*-*O*-esters react with albumin to form A α C-Cys³⁴ sulfenamide and sulfonamide adducts and also react with DNA to form dG-C8-A α C. HONH-A α C can undergo further oxidation by P450, by transition metals, or by oxygen to form NO-A α C and ROS. A redox cycling mechanism catalyzed by NADPH-P450 reductase can regenerate HONH-A α C (49, 64). The superoxide anion or other ROS can oxidize *S*-*N*-linked Cys-A α C to form the sulfenic and sulfonic acids of Cys³⁴ and Met residues of albumin.

the isotopic pair (*i.e.* for the radical cation (A α C^{•+} at *m/z* 183.1, [¹³C₆]A α C^{•+} at *m/z* 189.1) and protonated ions (A α C⁺ at *m/z* 184.1 and [¹³C₆]A α C at *m/z* 190.1)) (Fig. 3). Nine A α C-peptide adducts (P1–P9) were detected in the tryptic/chymotryptic digest. The assignments of the peptide adduct sequences and accurate mass measurements of the amino acid adducts, following digestion with Pronase E, leucine aminopeptidase, and prolidase, are listed in Table 1. Cys³⁴, followed by Tyr¹⁴⁰ and Tyr¹⁵⁰, formed adducts with HONH-A α C; an additional adduct was formed at Tyr³³² with *N*-acetoxy-A α C. The adduction of NO-A α C primarily occurred at Cys³⁴, followed by much lower levels of adduct formation at Tyr¹⁵⁰.

MS Characterization of Adducts Formed at Cys³⁴ of Albumin—The digestion of A α C-modified albumin with trypsin/chymotrypsin produced peptides containing adducts at ³¹LQQC*PF³⁶, ³²QQCPFEDHVK⁴¹ and ³¹LQQCPFEDHVK⁴¹.

A total of six adducts with different oxidation states of the sulfur atom were identified. The product ion spectra of several adducts peptides are described in detail below.

LQQ*CPFEDHVK-A α C Adducts—The single missed cleavage peptide containing the proposed sulfonamide adduct LQQ*C^[SO₂A α C]PFEDHVK (P2) (1555.7 Da), eluted at *t_R* = 17.7 min and occurred as a triply charged species [M + 3H]³⁺ at *m/z* 519.6 (Fig. 4A). The 213-Da increase in mass over the non-modified peptide corresponds to the addition of A α C (182 Da) and two oxygen atoms (32 Da) minus one proton (1 Da) on the -SH moiety. The product ion spectrum of *m/z* 519.6 displayed a series of *-b* ions and *-y* ions confirming the sequence assignment. The shift in masses at the **b*₄ and (**y*₈)²⁺ ions identify the site of adduction at the Cys³⁴ residue. The proposed sulfonamide adduct LQQ*C^[SOA α C]PFEDHVK (P3) (1539.7 Da) at *t_R* = 17.8 min occurred as a triply charged species [M + 3H]³⁺

Characterization of A α C-Serum Albumin Adducts

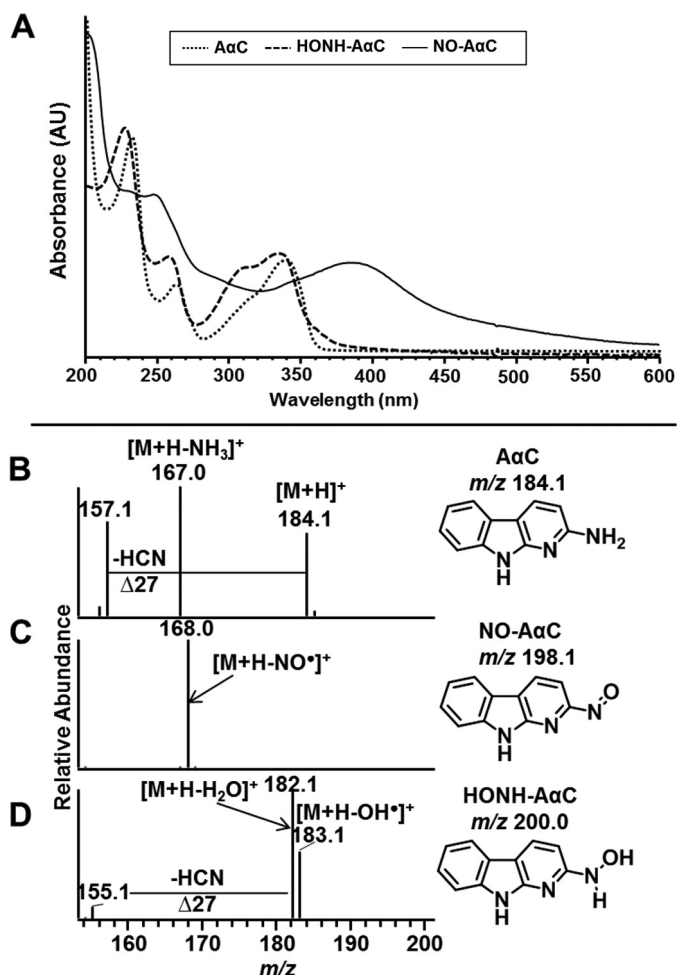


FIGURE 2. Characterization of A α C and its *N*-oxidized metabolites. A, UV spectra of A α C, NO-A α C, and HONH-A α C were obtained in methanol. Product ion spectra of A α C (B), NO-A α C (C), and HONH-A α C (D) were acquired by ion trap mass spectrometry.

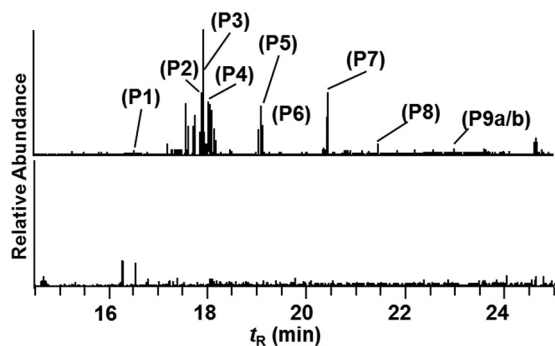


FIGURE 3. Mass tag data dependent MS² scanning of trypsin/chymotrypsin digest of albumin modified with a 50-fold molar excess of an equimolar mixture of *N*-acetoxy-A α C and *N*-acetoxy-¹³C₆A α C. Shown are reconstructed ion chromatograms for A α C at *m/z* 183.1 and 184.1 from digests of albumin modified with *N*-acetoxy-A α C/*N*-acetoxy-¹³C₆A α C (top) or digests of non-modified albumin (bottom). The chromatograms were acquired on ions exhibiting mass difference of *m/z* 6 (for singly charged ions), *m/z* 3 (for doubly charged ions), and *m/z* 2 (for triply charged ions). The ion intensities were normalized to the same scale.

at *m/z* 514.2, a mass 16 Da less than the sulfonamide adduct. The product ion spectrum of *m/z* 514.2 contains minor fragment ions at *m/z* 183.1 (A α C⁺) and 184.1 (A α C⁺), with a base peak at *m/z* 679.9, corresponding to the sulfonium ion

[M + 2H-A α C]²⁺ (Fig. 4B). The MS³ scan stage product ion spectrum of the proposed LQQ^{*}C^[SO]PFEDHVK sulfoxide ion at *m/z* 679.9 [M'] showed *-b* and *-y* ion series and supports the sequence assignment. Doubly charged product ion at *m/z* 648.9 attributed to the loss of CH₂SO from the M' ion and ^{*}b₄-SO, ^{*}b₅, ^{*}y₈, and ^{*}y₉ ions supports the proposed structure (Fig. 4C).

LQQ^{*}CPF-A α C Peptide Adducts—Three additional *S*-*N*-linked peptide adducts were identified. The product ion mass spectra of the doubly protonated ions are consistent with the A α C sulfonamide LQQ^{*}C^[SO₂A α C]PF (P4) ([M + H]⁺ at *m/z* 948.4, [M + 2H]⁺ at *m/z* 474.7, *t*_R = 17.9 min) (Fig. 4D), A α C sulfonamide LQQ^{*}C^[SOA α C]PF (P7) ([M + H]⁺ at *m/z* 932.4, [M + 2H]⁺ at *m/z* 466.7, *t*_R = 20.4 min) (Fig. 4, E and F), and A α C sulfenamide LQQ^{*}C^[A α C]PF (P8) ([M + H]⁺ at *m/z* 916.4, [M + 2H]⁺ at *m/z* 458.7 *t*_R 21.5 min) (Fig. 4G).

The doubly charged peptide precursor ion [M + 2H]²⁺ of LQQ^{*}C^[A α C]PF (P8) [M + H]⁺ at *m/z* 458.7 is a 181-Da increase in mass over the non-modified protonated peptide (*m/z* 735.3). This increase in mass corresponds to the addition of A α C (182 kDa) minus one proton (1 kDa) from the -SH moiety. The increase in mass of the peptide is consistent with the proposed sulfenamide linkage. The product ion spectrum of [M + 2H]²⁺ at *m/z* 458.7 (Fig. 4G) shows the *-b* ion and *-y* ion series, where ^{*}b₄, ^{*}y₃-^{*}y₅ ions provide evidence that adduction of A α C occurred at the sulfhydryl group of Cys³⁴. The product ion at *m/z* 439.3 (^{*}b₄-A α C-SH) occurs via the cleavage of the C-S bond (41, 42). The prominent base peak observed at *m/z* 184.1 is attributed to protonated A α C (Fig. 4G). It is noteworthy that most arylsulfenamide adducts undergo hydrolysis during proteolytic digestion, which generally makes these adducts difficult to detect (30, 43, 44).

MS Characterization of ^{*}Cys-A α C Adducts—The Cys sulfenamide- and sulfonamide-linked adducts of A α C underwent hydrolysis to produce A α C during proteolysis of albumin with Pronase E, leucine aminopeptidase, and prolidase. Two peaks attributed to Cys-A α C adducts containing the *S*-dioxide linkage were identified (*t*_R = 10.9 and 11.5 min) (A1) in the UPLC/MS chromatogram (Fig. 5, A and B). The precursor ions [M + H]⁺ were observed at *m/z* 335.0806, a value that is within 0.6 ppm of the calculated *m/z* value of the proposed sulfonamide structure (Table 1). The adducts were present in an approximate ratio of 4:6 in albumin modified with HONH-A α C and in a 2:8 ratio when albumin was modified with *N*-acetoxy-A α C; Fig. 5, A and B). The adducts were formed at ~5-fold higher levels in albumin treated with *N*-acetoxy-A α C than in albumin treated with HONH-A α C. The earlier eluting isomer underwent CID to preferentially form a radical cation at *m/z* 183.0790 (A α C^{•+}), whereas the second adduct favored the formation of the even electron ion at *m/z* 184.0867, the *m/z* of protonated ion of A α C⁺ (Fig. 5 (C and D) and Table 2). Other notable product ions were detected for both adducts but with different relative abundances: *m/z* 230.0382 ([A α C + SO]⁺); *m/z* 254.0922 ([M + H-NH₃-SO₂]⁺); *m/z* 271.1189 ([M + H-SO₂]⁺); and *m/z* 318.0547 ([M + H-H₂O]) (Fig. 5 (C and D) and Table 2).

Arylsulfonamides are weak acids, and the nitrogen anion of the sulfonamide linkage can form several tautomeric forms with hindered rotation about the S=N bond (45). However, the

TABLE 1
A α C-peptide and A α C-amino acid adducts identified using mass tag data-dependent acquisition

 Z, Charge state; t_R , retention time; M.W, molecular weight; 3-enzyme mixture, Pronase E, leucine aminopeptidase, and prolidase.

Peptide	Unlabeled (¹³ C ₆ labeled) Observed precursor ions (<i>m/z</i>)	Z	M.W	t_R (min)	A α C-peptide adduct	Site of modification	Enzyme
P1	481.9 (483.9)	3	1442.6	16.5	³² QQ*C ^[AαC] PFEDHVK ⁴¹ sulfonamide ^{a,b,c}	Cys ³⁴	
P2	778.9 (781.9)	2	1555.7	17.7	³¹ LQQ*C ^[AαC] PFEDHVK ⁴¹ sulfonamide ^{a,b,c}	Cys ³⁴	
	519.6 (521.6)	3					
P3	770.9 (773.9)	2	1539.7	17.8	³¹ LQQ*C ^[AαC] PFEDHVK ⁴¹ sulfonamide ^{a,b,c}	Cys ³⁴	
	514.2 (516.3)	3					
P4	948.4 (954.4)	1	947.4	17.9	³¹ LQQ*C ^[AαC] PF ³⁷ sulfonamide ^{a,b,c}	Cys ³⁴	Trypsin- chymotrypsin
	474.4 (477.4)	2					
P5	473.3 (476.3)	2	944.5	19.0	¹³⁹ L*Y ^[AαC] EIAR ^{144 a,b}	Tyr ¹⁴⁰	
P6	616.8 (619.8)	2	1231.5	19.3	³²⁷ LGM ^{oxi} FL*Y ^[AαC] EY ^{334 a,b}	Tyr ³³²	
P7	932.4 (938.4)	1	931.4	20.4	³¹ LQQ*C ^[AαC] PF ³⁷ sulfonamide ^{a,b,c}	Cys ³⁴	
	466.7 (469.7)	2					
P8	916.4 (922.4)	1	915.4	21.5	³¹ LQQ*C ^[AαC] PF ³⁷ sulfenamide ^{a,b,c}	Cys ³⁴	
	458.7 (461.7)	2					
P9(A,B)	517.3 (520.3)	2	1032.5	22.8	¹⁴⁹ F*Y ^[AαC] APELL ^{155a,b,c}	Tyr ¹⁵⁰	
Amino Acid	Unlabeled (¹³ C ₆ labeled) Observed precursor ions (<i>m/z</i>)	Z	M.W	t_R (min)	A α C-amino acid adduct	Site of modification	Enzyme
A1	335.0804 (341.0986)	1	335.1	10.9	*Cys ^[AαC] _{a,b}	Cys	
A2	363.1449 (369.1631)	1	363.2	11.8	*Tyr ^[AαC] _{a,b}	Tyr	3-Enzyme mixture
A3	361.1293 (367.1475)	1	361.1	12.1	*Tyr ^[AαC] _{a,b}	Tyr	

^a HONH-A α C/HONH-[¹³C₆] A α C-albumin-modified sample.

^b N-acetoxy-A α C/N-acetoxy-[¹³C₆] A α C-albumin-modified sample.

^c NO-A α C-modified sample.

prominent differences in the product ion spectra, combined with the inability to interconvert these Cys-A α C adducts at elevated temperature, suggest that the adducts are not conformational isomers.

The nitrenium ion of HONH-A α C can undergo charge delocalization to form the carbenium ion resonance form with electron deficiency centered at the C-3 position of the A α C skeleton (Fig. 5E) (46). We propose that one isomeric Cys-A α C adduct contains an S-N linkage, and the second adduct contains a thioether linkage, formed between the Cys³⁴-SH group and possibly the C-3 atom of A α C (46). The S-N-sulfenamide (or sulfonamide) and thioether adducts undergo oxidation, by ROS generated by aerobic oxidation of N-oxidized A α C metabolites (Fig. 1) or during proteolysis, to form the sulfonamide and sulfone linkages (Fig. 5E) (47). Both adducts undergo CID to form the proposed sulfonium ion at *m/z* 230.0385 (Fig. 5E). These adducts were not chromatographically resolved in the tryptic/chymotryptic digests of albumin. Large scale syntheses and NMR studies are required to elucidate the respective structures of these A α C-Cys-S-dioxide linked isomers. The Cys³⁴ of albumin was reported to react with N-acetyl-p-benzoquinoneimine, the electrophilic metabolite of acetaminophen, and formed two regioisomeric adducts (42).

MS Characterization of Adducts Formed at Tyr¹⁴⁰, Tyr¹⁵⁰, and Tyr³³² of Albumin—Three adducts were formed between Tyr residues of albumin and A α C (Table 1).

L*YEIAR Peptide Adduct—The product ion spectrum of the L*YEIAR (P5) adduct with a doubly charged peptide precursor ion [M + 2H]²⁺ at *m/z* 473.3 (t_R = 14.1 min) displayed a series of -*b* ions and -*y* ions, which identifies the sequence as ¹³⁹L*Y^[A α C]EIAR¹⁴⁴, with the site of adduction at Tyr¹⁴⁰ (Fig. 6A). The ion at *m/z* 763.4 is proposed to arise by the loss of A α C as a radical cation at *m/z* 183.1 [M + H-A α C]⁺, followed by the neutral loss of quinone methide (106.1 Da) [M + H-A α C-C₇H₆O]⁺ to form the ion at *m/z* 657.4 (Fig. 6B). The mass spectral data support the proposed structure as an O-linked adduct formed between oxygen atom of Tyr and possibly the C-3 atom of the heterocyclic skeleton of A α C (46). Further support for the proposed O-linkage is provided by the lower region of the HCD mass spectrum; ions are observed at *m/z* 183.0790 (*m/z* 183.0791, calculated) and *m/z* 199.0745 (*m/z* 199.0741, calculated) and attributed to [A α C]⁺ and [A α C+O]⁺, respectively (Fig. 6, A and B). We recently reported a similar mechanism of fragmentation of an O-linked adduct formed between tyrosine and the HAA 2-amino-1-methyl-6-phenylimidazo[4,5-*b*]pyridine (PhIP) (32).

MS characterization of an O-Linked Tyr-A α C Adduct—The proteolysis of albumin adducts with Pronase E, leucine aminopeptidase, and prolidase produced two Tyr linked adducts of A α C. A first set of Tyr-A α C and Tyr-[¹³C₆]A α C adducts (A2) was observed at *m/z* 363.1449 (*m/z* 363.1451, calculated) and *m/z* 369.1629 (*m/z* 369.1631, calculated) at t_R 11.8 min. The product ion spectrum of the unlabeled Tyr-A α C adduct

Characterization of A α C-Serum Albumin Adducts

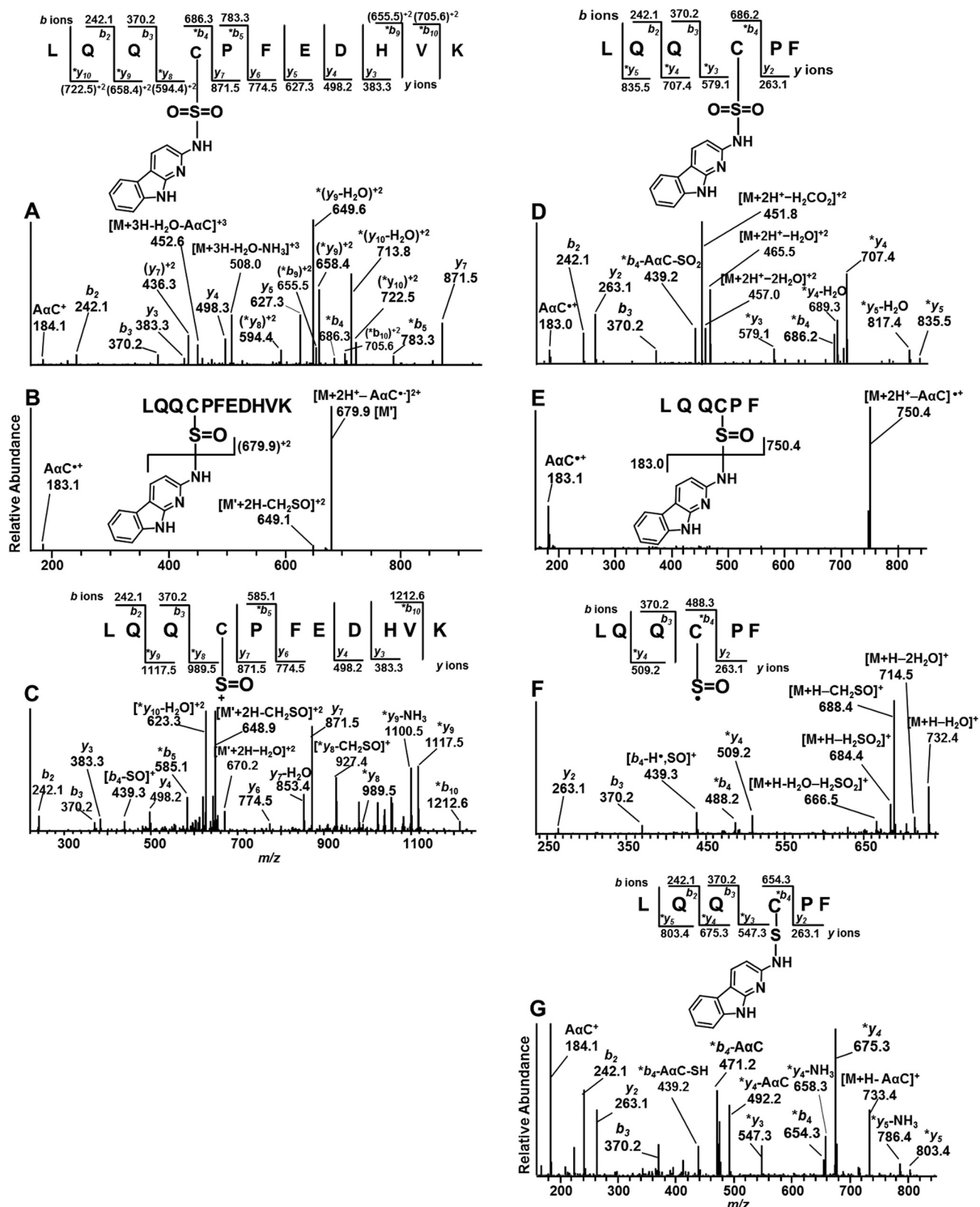


FIGURE 4. A and B, product ion spectra of A α C adducts of LQQC^[SO₂A α C]PFEDHVK (P2) $[M + 3H]^3+$ at m/z 519.6 (A) and LQQC^[SO₂A α C]PFEDHVK (P3) $[M + 3H]^3+$ at m/z 514.2 (B). C, consecutive reaction monitoring at the MS³ scan stage of LQQC^[SO₂A α C]PFEDHVK (P3) targeting m/z 514.2 product ion from second generation product ion spectrum of m/z 514.2. D, LQQC^[SO₂A α C]PF (P4) $[M + 2H]^2+$ at m/z 474.7. E, LQQC^[SO₂A α C]PF (P7) $[M + 2H]^2+$ at m/z 466.7. F, third generation product ion spectrum of $[M + 2H]^2+$ at m/z 466.7. G, LQQC^[A α C]PF (P8) $[M + 2H]^2+$ at m/z 658.7 of the trypsin/chymotrypsin digest of albumin modified with N-acetoxy-A α C and N-acetoxy-[¹³C]₆A α C. *, fragment ions with A α C adduction.

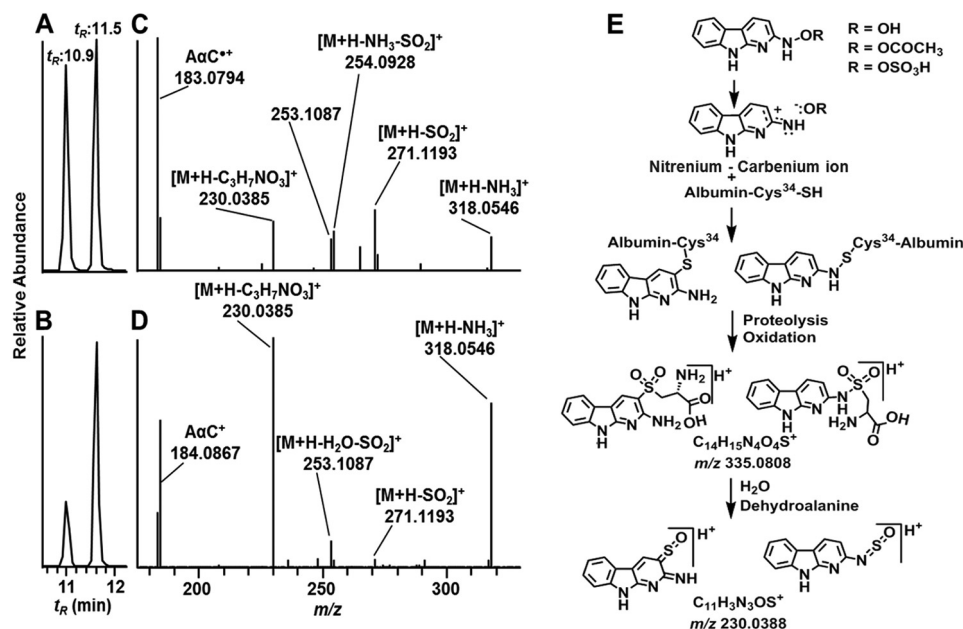
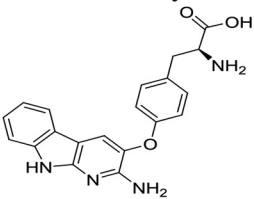
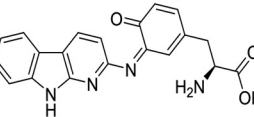
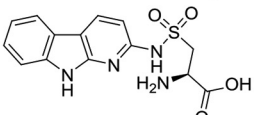
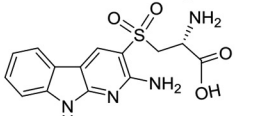


FIGURE 5. AαC-Cys S-dioxide adducts of albumin obtained from Pronase E/prolidase/leucine amino peptidase digest of albumin modified with HONH-AαC and HONH-[¹³C₆]AαC or N-acetoxy-AαC and N-acetoxy-[¹³C₆]AαC. Shown is a total ion chromatogram (TIC) at the MS² scan stage of [M + H]⁺ at *m/z* 335.0806 obtained from albumin modified with HONH-AαC (A) and N-acetoxy-AαC (bottom) (B). The product ion spectra of [M + H]⁺ at *m/z* 335.0806 of C[¹³SO₂AαC] at 10.9 min (C) and at 11.5 min (D) and proposed structures of isomers are shown. E, proposed formation of cysteine-S-yl-dioxide-AαC isomeric adducts by reaction of Cys with the nitrenium-carbenium ion resonance forms of HONH-AαC and CID fragmentation mechanism of sulfonium ion at *m/z* 230.0385 in product ion spectra of isomers ([M + H]⁺ at *m/z* 335.0806).

TABLE 2

Accurate mass measurements of AαC amino acid adducts formed with Tyr and Cys

AαC-amino acid adduct	Precursor ion/product ion assignment	Observed <i>m/z</i>	Molecular Formula	Calculated <i>m/z</i>	Error ppm
AαC-O-Tyr 	[M+H] ⁺	363.1449	C ₂₀ H ₁₉ N ₄ O ₃	363.1451	0.5
	[M+H-H ₃ N] ⁺	346.1184	C ₂₀ H ₁₆ N ₃ O ₃	346.1186	0.5
	[M+H-CH ₂ O ₂] ⁺	317.1392	C ₁₉ H ₁₇ N ₄ O	317.1396	1.0
	[M+H-CH ₃ NO ₂] ⁺	302.1285	C ₁₉ H ₁₆ N ₃ O	302.1287	0.7
	[M+H-C ₂ H ₅ NO ₂] ⁺	288.1129	C ₁₈ H ₁₄ N ₃ O	288.1131	0.7
	[M+H-C ₉ H ₁₁ NO ₂] ⁺	198.0659	C ₁₁ H ₈ N ₃ O	198.0662	1.0
	[M+H-C ₉ H ₁₀ NO ₃] ⁺	183.0789	C ₁₁ H ₉ N ₃	183.0791	1.1
AαC-N=Tyr 	[M+H] ⁺	361.1293	C ₂₀ H ₁₇ N ₄ O ₃	361.1295	0.6
	[M+H-H ₃ N] ⁺	344.1025	C ₂₀ H ₁₄ N ₃ O ₃	344.1029	1.1
	[M+H-CH ₂ O ₂] ⁺	315.1239	C ₁₉ H ₁₅ N ₄ O	315.1240	0.7
	[M+H-CH ₃ NO ₂] ⁺	300.1130	C ₁₉ H ₁₄ N ₃ O	300.1131	0.7
	[M+H-C ₂ H ₅ NO ₂] ⁺	288.1129	C ₁₈ H ₁₄ N ₃ O	288.1137	2.8
	[M+H-C ₉ H ₇ NO ₃] ⁺	183.0789	C ₁₁ H ₉ N ₃	183.0791	1.1
	[M+H-C ₉ H ₇ NO ₃] ⁺	184.0868	C ₁₁ H ₁₀ N ₃	184.0869	0.5
AαC-HN-SO₂-Cys 	[M+H] ⁺	335.0804	C ₁₄ H ₁₅ N ₄ O ₄ S	335.0808	1.2
	[M+H-H ₃ N] ⁺	318.0546	C ₁₄ H ₁₂ N ₃ O ₄ S	318.0548	1.2
	[M+H-O ₂ S] ⁺	271.1193	C ₁₄ H ₁₅ N ₄ O ₂	271.1190	0.4
	[M+H-H ₃ NO ₂ S] ⁺	254.0928	C ₁₄ H ₁₂ N ₃ O ₂	254.0924	-1.5
AαC-SO₂-Cys 	[M+H-C ₃ H ₁₂ NO ₃] ⁺	230.0385	C ₁₁ H ₃ N ₃ OS	230.0384	0.3
	[M+H-C ₃ H ₅ O ₄ NS] ⁺	184.0867	C ₁₁ H ₁₀ N ₃	184.0869	1.0
	[M+H-C ₃ H ₆ O ₄ NS] ⁺	183.0790	C ₁₁ H ₉ N ₃	183.0791	0.5

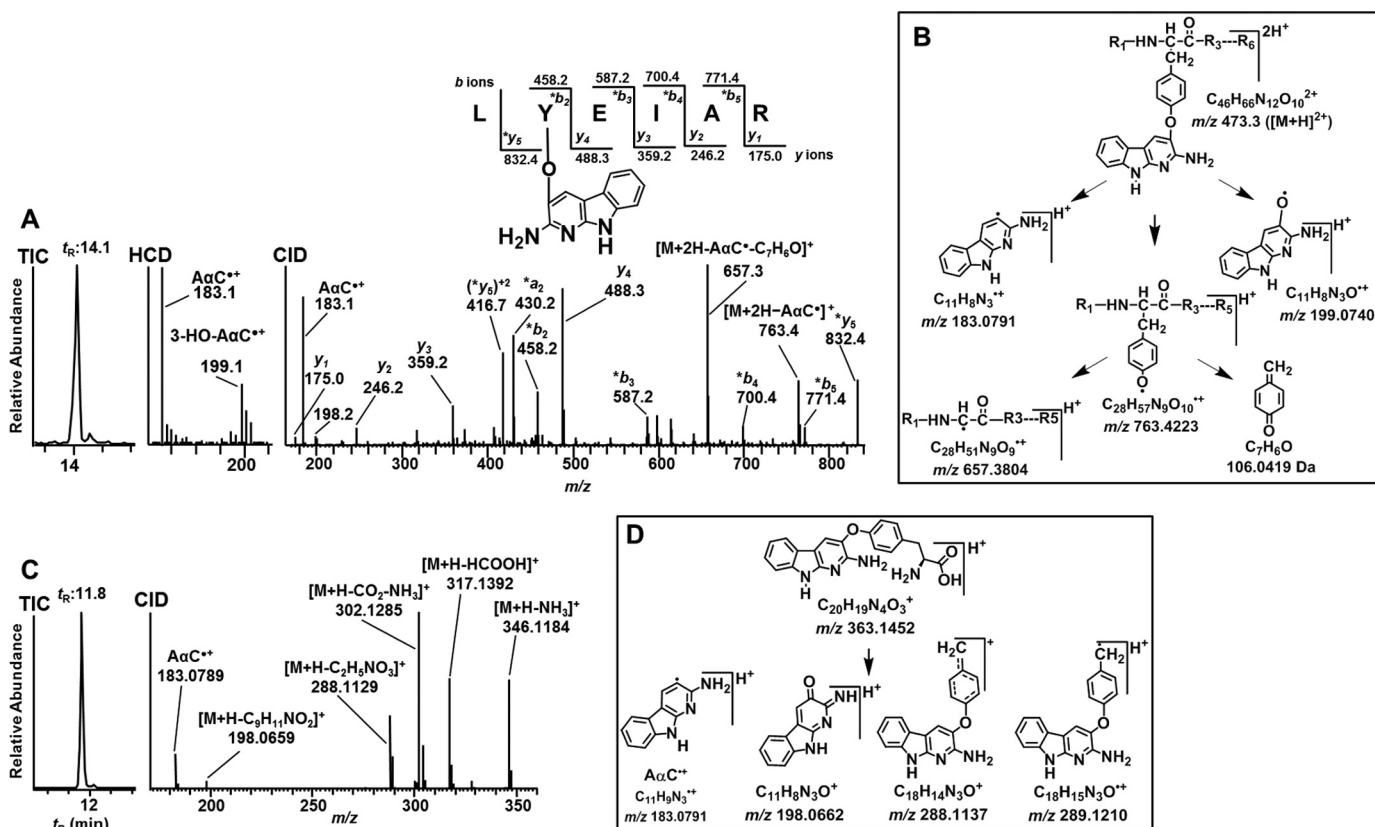


FIGURE 6. Product ion spectrum of A α C-Tyr peptide and amino acid adduct of albumin modified with *N*-acetoxy-A α C and *N*-acetoxy- $^{13}C_6$ A α C. Shown are TIC, HCD, and CID product ion spectra of LY $^{[A\alpha C]}$ EIAR (P5) $[M + 2H]^{2+}$ at m/z 473.3, $t_R = 14.1$ min (A), and proposed CID fragmentation mechanism of LY $^{[A\alpha C]}$ EIAR (P5) adduct $[M + 2H]^{2+}$ at m/z 473.3 (B). Shown are TIC (C) and product ion spectrum (D) of amino acid adduct $[M + H]^+$ at m/z 363.1449 (A2) at $t_R = 11.8$ min and proposed CID fragmentation mechanism of A α C-Tyr adducts $[M + H]^+$ at m/z 363.1452 (E).

$[M + H]^+$ at m/z 363.1449 displayed fragment ions at m/z 346.1186, 317.1395, and 302.1285 attributed to the losses of NH_3 , H_2CO_2 , and NH_3 and CO_2 , respectively (Fig. 6C and Table 2). The product ions at m/z 289.1210 $[M + H-C_2H_5NO_2]^+$ and 288.1137 $[M + H-C_2H_4NO_2]^+$ are proposed to arise by cleavage of the C^α and C^β bond of tyrosine. The fragment ion at m/z 183.0791 is assigned to A αC^+ , and the ion at m/z 198.0659 is tentatively assigned as the protonated ion of the 2-imino-3-oxo derivative of A α C, with the loss of phenylalanine (165.0790 Da) as a neutral fragment. The ion at m/z 198.0659 provides evidence that adduct formation occurred between the 4-HO group of tyrosine and the A α C heterocyclic ring (Fig. 6D).

F*YAPPELL-A α C Adducts—Two minor Tyr adducts of A α C with the peptide sequence $^{149}F^*Y^{[A\alpha C]}APELL^{155}$ (P9A and P9B; Fig. 3 and Table 1) were identified at t_R 14.5 and 15.8 min (Fig. 7A). The full scan spectra of both adducts displayed doubly charged $[M + 2H]^{2+}$ at m/z 517.3. The CID fragment ions of m/z 517.3 displaced the same characteristic $-b$ ion and $-y$ ion series attributed to the $F^*Y^{[A\alpha C]}APELL$ for both peptide adducts (Fig. 7A, CID). The shift in mass between the y_5 and y_6 ion series proves that the site of A α C adduction occurred at Tyr 150 for both peptides (Fig. 7A). CID did not provide appreciable fragment ions at the low m/z region for either adduct. The doubly protonated ions $[M + 2H]^{2+}$ at m/z 517.3 were subjected to HCD to examine for potential fragmentation of the bond formed between the Tyr and A α C. The extracted

ion chromatograms were generated at m/z 183.0791 and m/z 184.0869 (Fig. 7A, HCD). The earlier eluting adduct (P9A) at $t_R = 14.5$ min displayed a prominent fragment ion at m/z 184.0869, an ion attributed to protonated A α C (Fig. 7A, HCD at $t_R = 14.5$). The linkage of this adduct may have occurred between the C-3 or C-5 atom of the Tyr phenyl ring and the exocyclic amino group of A α C. The HCD product ion spectrum of the second adduct (P9C) at $t_R = 15.8$ min showed a mixture of product ions assigned as the radical cation of A αC^+ and protonated A α C, respectively, at m/z 183.0789 and m/z 184.0868 (Fig. 7A, HCD at $t_R = 15.8$). A Tyr linkage may have formed at the C-3 or C-7 atom of the heterocyclic ring of A α C, based on studies of nucleophilic trapping agents adducting at these sites of the nitrenium ion of A α C (46, 48).

MS Characterization of an Amine-linked A α C Tyr Adduct—The second set of Tyr-A α C and Tyr- $^{13}C_6$ A α C adducts (A3) eluted at $t_R = 12.1$ min (Fig. 7B). The protonated ions $[M + H]^+$ were observed at m/z 361.1293 and 367.1475, respectively, a mass 2 Da less than the Tyr-A α C and Tyr- $^{13}C_6$ -A α C adducts (m/z 363.1449 and 369.1631) described above (Fig. 7B and Table 2). The structure of the adduct is proposed to be a quinoneimine-linked adduct, which occurs by oxidation of P9A (Fig. 7B) during proteolytic digestion with the three-enzyme mixture. The product ion spectrum of $[M + H]^+$ at m/z 361.1293 shows ions at m/z 344.1025, 315.1239, and 300.1130, which are of losses of NH_3 , H_2CO_2 , and NH_3 and CO_2 , respec-

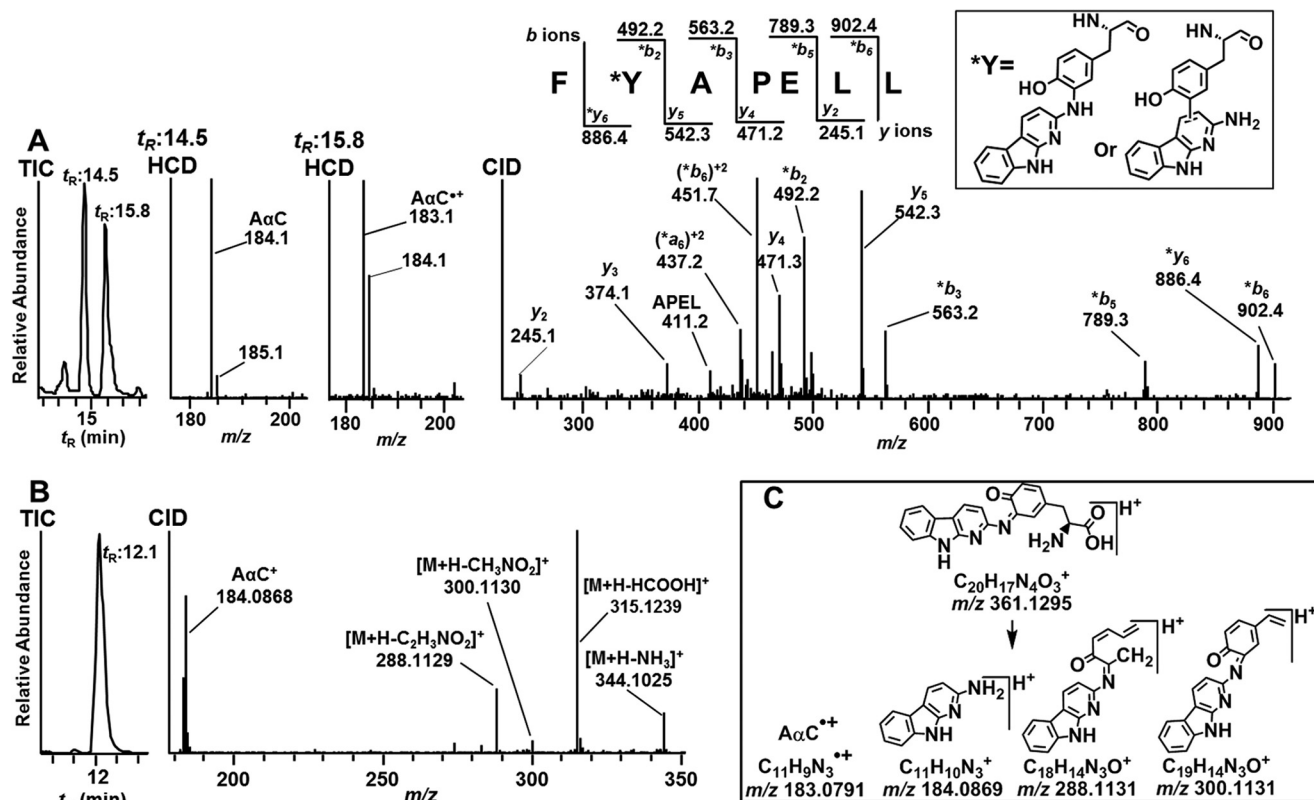


FIGURE 7. Characterization of isomeric FY^[A α C]PELL peptides and an A α C-amine-linked Tyr amino acid adduct of albumin modified with *N*-acetoxy-A α C and *N*-acetoxy-[¹³C₆]A α C. **A**, TIC, HCD, and CID product ion spectra of FY^[A α C]PELL (P9) [M + 2H]²⁺ at m/z 517.3, t_R = 14.5 and 15.8 min (CID spectra for both peptides were identical; only the spectrum of peptide at t_R 14.5 min is shown). **B**, TIC and CID product ion spectra of A α C-amine-linked Tyr amino acid adduct [M + H]⁺ at m/z 361.1299 (A2) at t_R 12.1 min. **C**, proposed CID fragmentation mechanism of A α C-Tyr adduct [M + H]⁺ at m/z 361.1299. *, fragment ions with A α C adduction.

tively (Fig. 7B and Table 2). The product ion at m/z 288.1129 is proposed to arise following ring opening of the protonated quinoneimine ring (Fig. 7C). The Tyr-[¹³C₆]A α C adduct displays the same product ions as the unlabeled adduct but shifted by 6 m/z .

A third peptide adduct formed between A α C and Tyr was observed only in the albumin modified with *N*-acetoxy-A α C. The CID-MS/MS spectrum of doubly charged protonated precursor ion at m/z 616.8 at 19.3 min displayed a typical *-b* and *-y* ion pattern attributable to LGMFL*Y^[A α C]EY (P6) with A α C adduction at Tyr³³² (supplemental Fig. S1, top). The [¹³C₆]A α C homologue of this adduct at m/z 619.8 displayed the same pattern of fragmentation (supplemental Fig. S1, bottom).

A α C-SA Adduct Formation as a Function of Concentration of *N*-Oxidized A α C Metabolites—The LQQ*C^[SOA α C]PFEDHVK (P3) sulfonamide adduct at Cys³⁴ accounted for 73–80% of the total ion counts of A α C-peptide adducts, when commercial albumin was reacted with a 50-fold molar excess of *N*-oxidized A α C metabolites. *In vivo*, the exposure to A α C occurs at much lower levels than the physiological concentration of albumin, and relative abundances of adducts formed may be different from those adducts formed at elevated exposures to A α C *in vitro*. Therefore, albumin was treated with HONH-A α C or *N*-acetoxy-A α C over a million-fold range of carcinogen/mol of albumin (1–10⁻⁶) (Fig. 8, A and B). We also examined the effect of plasma matrix components on the reactivity of albumin with *N*-oxidized A α C metabolites. Representative UPLC/MS chro-

matograms of the peptide adducts recovered from commercial albumin or albumin in plasma modified with 1 molar eq of *N*-acetoxy-A α C are shown in supplemental Fig. S2, A and B.

The Tyr-peptide adducts of A α C at Tyr¹⁴⁰, Tyr¹⁵⁰, and Tyr³³² residues were only detected when albumin was reacted with ≥ 0.01 mol *N*-acetoxy-A α C per mol albumin. In contrast, adducts were still formed at Cys³⁴ with a 1×10^{-5} molar ratio of *N*-acetoxy-A α C/albumin (Fig. 8, A and B), and LQQ*C^[SOA α C]PFEDHVK sulfonamide was the major adduct. The amounts of A α C-peptide adducts formed were ~ 5 –40 times higher in reactions of albumin conducted with *N*-acetoxy-A α C than those amounts of albumin adducts formed with HONH-A α C (Fig. 8, A and B). The level of A α C adduct formation with albumin in plasma was severalfold lower than adduct levels formed with commercial albumin (data not shown). Plasma albumin adducts were not detected at Tyr¹⁴⁰, Tyr¹⁵⁰, or Tyr³³² residues at any concentration of *N*-oxidized A α C, and the sulfonamide LQQ*C^[SOA α C]PFEDHVK was the predominant adduct.

A α C-DNA and A α C-Albumin Adduct Formation in Human Hepatocytes—Reactive *N*-oxidized intermediates of A α C are formed and adduct to DNA in human hepatocytes and albumin in human hepatocytes (Fig. 1) (20, 33). The basal activities of P450 1A1 and 1A2, two major isoforms involved in *N*-oxidation of A α C (16, 17), were measured in human hepatocytes from three donors using ethoxyresorufin and methoxyresorufin as substrates (33). The level of dG-C8-A α C adduct formation

Characterization of A α C-Serum Albumin Adducts

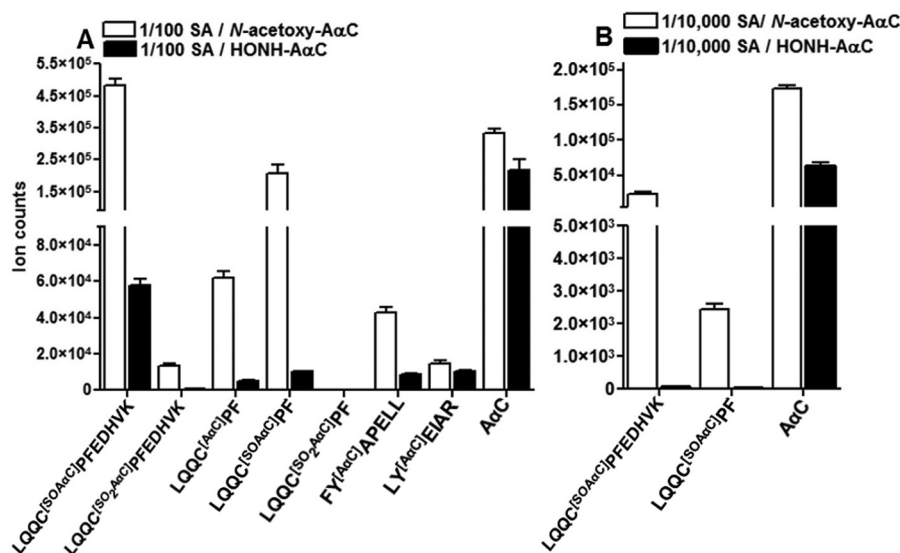


FIGURE 8. Ion counts of A α C-peptide adducts targeting Cys³⁴ and Tyr¹⁴⁰ Tyr¹⁵⁰ and free A α C recovered from trypsin/chymotrypsin digests of albumin modified with 1/10⁻² molar eq of HONH-A α C or N-acetoxy-A α C, 0.3 μ g digest/injection (A) and albumin modified with 1/10⁻⁴ molar eq of HONH-A α C or N-acetoxy-A α C, 1.0 μ g of digest/injection (B). Data are plotted as mean and S.D. (error bars) of ion counts ($n = 3$).

from the two donors (A and C) with the highest P450 1A1 and 1A2 activities produced higher levels of dG-C8-A α C than donor B with low enzyme activity (Fig. 9A).

The mass chromatograms of A α C-albumin peptide adducts, following tryptic/chymotryptic digestion of albumin recovered from hepatocytes, are shown in Fig. 9B. The relative ion abundances of the peptide adducts are summarized in Fig. 9C, and product ion spectra are presented in supplemental Fig. S3. The major adduct, based on ion counts, is LQQ*C^[SOA α C]-PFEDHVK sulfonamide, followed by LQQ*C^[SOA α C]PF and LQQ*C^[A α C]PF. The occurrence of the LQQ*C^[SOA α C]-PFEDHVK as the major adduct in hepatocytes is similar to the findings of commercial albumin and albumin in plasma treated with N-oxidized A α C metabolites (Figs. 7A, 8A, and 9 (B and C)). The LQQ*C^[A α C]PF sulfenamide and LQQ*C^[SOA α C]PF sulfonamide were also identified but occurred at lower ion abundances (Fig. 9 (B and C) and supplemental Fig. S3 (A–C)). LQQ*C^[SO2A α C]PF and LQQ*C^[SO2A α C]PFEDHVK were not detected.

In the absence of stable, isotopically labeled internal standards, quantitative peptide adduct measurements and correlations to DNA adduct levels of A α C cannot be determined. However, the ion counts of the major albumin peptide adduct, LQQ*C^[SOA α C]PFEDHVK sulfonamide, were greatest in donor C, who also harbored the highest level of dG-C8-A α C (Fig. 9, A–C). Very high levels of A α C also were recovered in all of the hepatocytes (Fig. 9, B and C). The occurrence of A α C is attributed to hydrolysis of S-N-linked albumin-A α C adducts during proteolysis and not to unmetabolized A α C bound to albumin, because the isolation procedure effectively removed all unbound A α C from albumin in the cell culture media.³

Oxidative Status of Albumin-Cys³⁴ and Albumin-Met³²⁹ in Human Hepatocytes Exposed to A α C—N-Oxidized metabolites of arylamines generate ROS (49). We sought to determine if

A α C had induced oxidative stress in hepatocytes by identification of oxidation products of Cys³⁴ and Met residues of albumin (50–52). The oxidized sulfinic LQQ*C^[SO2H]PF and sulfonic LQQ*C^[SO3H]PFEDHVK acids of Cys³⁴ of albumin were monitored (29, 32), and LQQCPF was measured following derivatization of albumin with IAM (29). Elevated levels of the protonated [M + H]²⁺ peptides for LQQ*C^[SO2H]PFEDHVK at m/z 688.3 and LQQ*C^[SO3H]PFEDHVK at m/z 696.3 (29) were detected in all three sets of hepatocytes treated with A α C (Fig. 9D). The product ion spectra at m/z 688.3 and 696.3 displayed typical *-b* and *-y* ion series type fragment ions (supplemental Fig. S4, A and B) and permitted the assignments as the peptide sequences of the Cys sulfinic and sulfonic acids (29). The levels of LQQ*C^[SO2H]PFEDHVK and LQQ*C^[SO3H]PFEDHVK in A α C/[¹³C₆]A α C-treated hepatocytes were 6–8 and 4–6 times higher, respectively, than the levels in untreated controls, and the levels of IAM-derivatized LQQ*CPF were decreased by more than 10-fold in A α C-treated hepatocytes (Fig. 9, B and D). A Myrimatch search for oxidation sites in albumin also identified oxidation at the Met³²⁹ residue of albumin. The product ion spectrum of trypsin/chymotryptic peptide DVFLGM^[O]F at [M + H]⁺ at m/z 844.4 representing Met³²⁹ oxidation resulted in typical *-b* and *-y* types of fragment ions, where *-*y*₂-**y*₆ and *-*b*₆ product ions further confirmed oxidation at Met³²⁹ (supplemental Fig. S4C). From targeted analysis, the level of DVFLGM^[O]F was ~6 times higher in A α C/[¹³C₆]A α C-treated hepatocytes than in untreated hepatocytes (Fig. 9, B and D).

Discussion

Primary human hepatocytes are an ideal *ex vivo* model system for studying metabolism, bioactivation, and mechanisms of toxicity of carcinogens, because cofactors are present at physiological concentrations, and biotransformation pathways may closely simulate those that occur *in vivo* (53). In this study, we investigated the metabolic activation of A α C, a rodent liver carcinogen, in human hepatocytes and examined the reactivity of its genotoxic N-oxidized metabolites of A α C with DNA and

³ K. Phatak, unpublished observations.

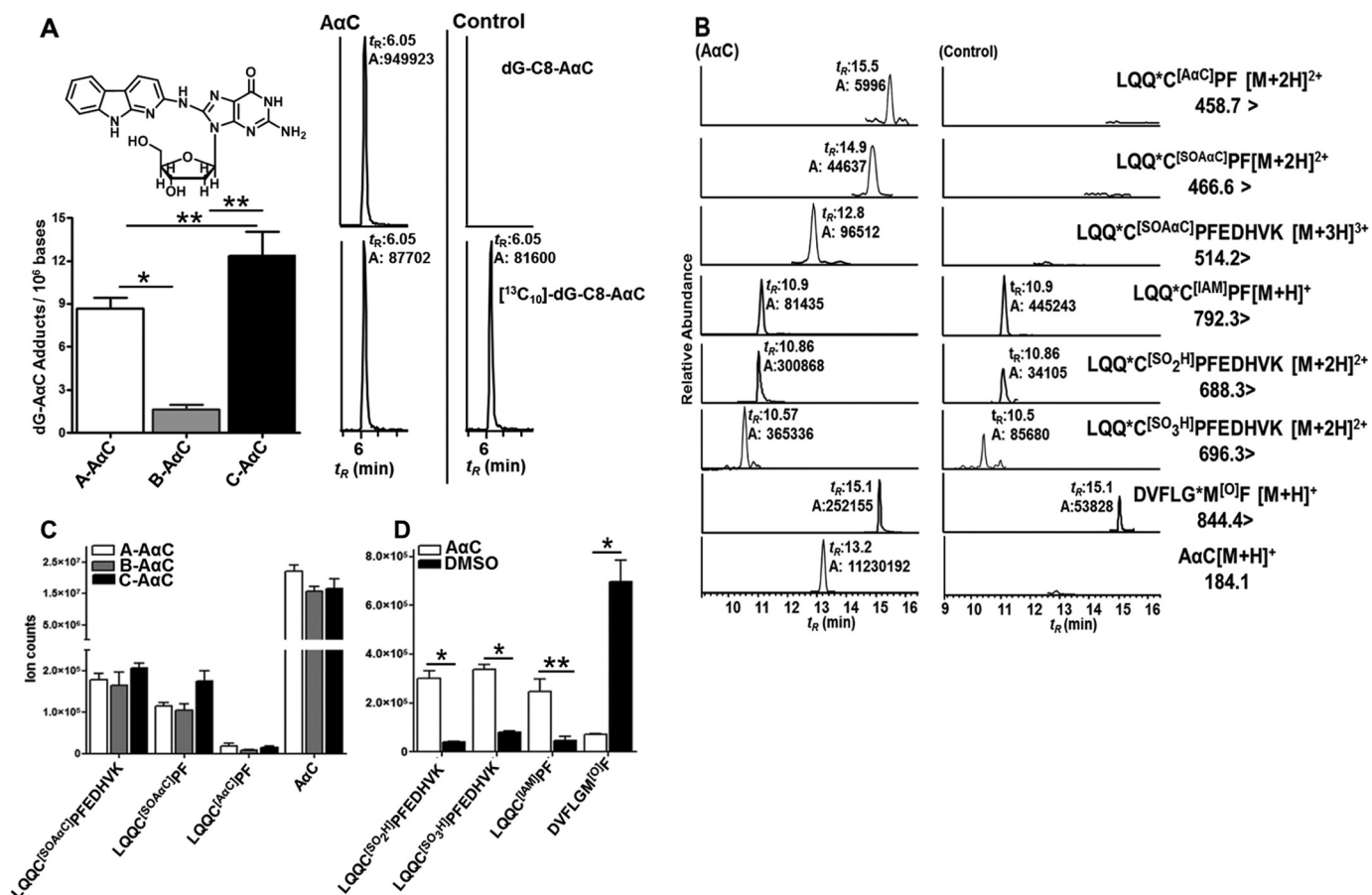


FIGURE 9. *A*, estimates of dG-C8-A α C adduct formation in hepatocytes of donors A, B, and C treated with 50 μ M A α C. Shown are UPLC-MS³ chromatograms of dG-C8-A α C from hepatocytes treated with 50 μ M A α C and with DMSO (control). For dG-C8-A α C, ions at m/z 449.1 (MS^1) > 333.1 (MS^2) > 209.2, 291.4, 316.4 (MS^3) (top) and for the internal standard, [¹³C₁₀]dG-C8-A α C, ions at m/z 459.1 (MS^1) > 338.1 (MS^2) > 210.2, 295.4, 321.5 (MS^3) (bottom) were monitored. *B*, UPLC-ESI/MS² chromatograms of A α C-peptide adducts and Cys and Met oxidation products recovered from trypsin/chymotrypsin digests of albumin from hepatocytes of donor A treated with A α C and [¹³C₆]A α C (50 μ M) and donor A treated with DMSO (control). Shown are ion counts of A α C-peptide adducts and A α C (C) and Cys³⁴ sulfonic acid, Cys³⁴ sulfenic acid, Met^{32/33} sulfoxide, and LQQC³⁴PF alkylated with IAM obtained from trypsin/chymotrypsin digests of albumin of hepatocytes of donor A, B and C treated with a 50 μ M equimolar mixture of A α C and [¹³C₆]A α C for 24 h or treated with DMSO (control) (*D*). Values are reported as the mean and S.D. (error bars) ($n = 3$). *, $p < 0.01$ using one-way ANOVA for donors A, B, and C treated with 50 μ M A α C; **, $p < 0.05$ for comparison between donors A and B and donors B and C using Tukey's multiple-comparison test for DNA adducts. *, $p < 0.01$; **, $p < 0.05$, A α C-treated versus control (DMSO-treated) (two-tailed Student's t test) for peptide adducts.

albumin. Our goal is to develop and implement albumin-based biomarkers of A α C and other HAAs in molecular epidemiological studies designed to assess the role of HAAs in human cancers (54). The Cys³⁴ residue was the major nucleophilic site of albumin to form adducts with A α C, followed by Tyr¹⁴⁰ and Tyr¹⁵⁰, which formed adducts at minor levels. Another HAA, PhIP (55), also primarily formed adducts at the Cys³⁴ of albumin with considerably lower levels of adducts occurring at Tyr¹⁴⁰ and Tyr¹⁵⁰ (56). In contrast, the Tyr¹⁴⁰ and Tyr¹⁵⁰ residues of albumin are the preferred site for adduct formation of neurotoxic organophosphate compounds (57–59).

The preliminary characterization A α C-albumin adducts was performed *in vitro*. The formation of A α C-albumin adducts was greatly enhanced by the *in situ* generation of *N*-acetoxy-A α C, a reactive intermediate of HONH-A α C, which undergoes heterolytic cleavage to produce the nitrenium ion (48). *N*-Acetoxy-A α C is a penultimate metabolite of A α C that adducts to DNA and proteins (17). The *N*-acetoxy intermediates of HONH-A α C and other *N*-hydroxylated HAAs, such as 2-hydroxyamino-3-methylimidazo[4,5-*f*]quinoline and 2-hydroxyamino-3,8-

dimethylimidazo[4,5-*f*]quinoxaline, are unstable and cannot be isolated (60). However, the *in situ* formation of these *N*-acetoxy intermediates in the presence of DNA, by reaction of the *N*-hydroxylated HAAs with acetic anhydride, increased the levels of DNA adducts by 10–30-fold (36, 61, 62). Using a similar reaction scheme, we showed that adduct formation of HONH-A α C with albumin was also greatly enhanced by the *in situ* generation of *N*-acetoxy-A α C (Fig. 8, *A* and *B*). The Lys, Arg, Cys, and Tyr residues of albumin can potentially compete with HONH-A α C and undergo acetylation with acetic anhydride and influence the formation of different A α C-albumin adducts. However, the same A α C-albumin adducts were formed by reaction of albumin with a 50-fold molar excess of HONH-A α C, NO-A α C, or *N*-acetoxy-A α C generated *in situ* (Table 1). Moreover, the Myrimatch search engine did not detect acetylation at Lys, Arg, Cys, or Tyr residues of albumin under these reaction conditions (100 mM potassium phosphate buffer (pH 7.4, 37 °C)). Under low reaction conditions with HONH-A α C (10,000:1, albumin/HONH-A α C), the levels of Cys³⁴ adducts were 50-fold greater when albumin was reacted with HONH-

Characterization of A α C-Serum Albumin Adducts

A α C in the presence of acetic anhydride than by reaction of albumin with HONH-A α C alone, thereby demonstrating that *N*-acetoxy-A α C is efficiently formed *in situ* and readily reacts with nucleophilic sites of albumin to form covalent adducts (Fig. 8, A and B).

Human hepatocytes efficiently bioactivated A α C to electrophilic *N*-oxidized metabolites, which formed covalent adducts with DNA and albumin (Fig. 9). The DNA adduct, dG-C8-A α C, was formed at relatively high levels, ranging from 2 to 12 adducts/10⁶ DNA bases, consistent with our previous data (20, 33). dG-C8-A α C was also previously identified in salivary DNA of smokers (63). The Cys³⁴ residue was the sole site of albumin found to form adducts with A α C metabolites in hepatocytes; both sulfenamide and sulfinamide adducts were identified. However, the ion counts of A α C recovered from the albumin digest were 100-fold or greater than the ion counts of any of the A α C-Cys adducts. These findings signify that a large proportion of the *S*-*N*-linked albumin-A α C adducts underwent hydrolysis during proteolysis. In the absence of stable peptide adducts or isotopically labeled LQQ*C^[SO α A α C]PFEDHVK peptides for internal standards, it is difficult to determine the relative reactivity of *N*-oxidized A α C metabolites with DNA and albumin in hepatocytes.

HONH-A α C and NO-A α C undergo redox cycling in hepatocytes and produce ROS (Fig. 1) (49, 64). Previous studies reported that structurally related aromatic amines, some of which are present in tobacco smoke (1, 66), deplete glutathione levels in the liver or *ex vivo* in hepatocytes of rodents and induce oxidative DNA damage (67–69); however, the oxidation of albumin was not reported in those studies. In our study, we show that albumin scavenges ROS produced by metabolites of A α C in human hepatocytes by formation of the oxidized Cys³⁴-containing peptides LQQ*C^[SO 2 H]PFEDHVK, LQQ*C^[SO 3 H]PFEDHVK, and the methionine oxidation peptide DVFLGM^{[O]F}. The level of Cys³⁴ of albumin alkylated with IAM prior to proteolytic digestion decreased by more than 90% in hepatocytes treated with A α C and provides strong evidence that Cys³⁴ of albumin is scavenging ROS (Fig. 9C). Together with Cys³⁴, six Met residues of albumin display antioxidant activity toward O₂⁻, H₂O₂, and HOCl (51, 52). Met³²⁹ was the primary site of Met oxidation in albumin from human hepatocytes treated with A α C. The oxidation of Met residues, particularly Met³²⁹, has been observed in albumin of hemodialysis patients (52).

The major adducts of A α C formed with albumin were determined in human hepatocytes by employing data-dependent scanning and bottom-up proteomics approaches, and the adduction products were the same as those adducts formed *in vitro* with commercial albumin reacted with *N*-oxidized A α C intermediates. The dose of A α C (50 μ M) employed in human hepatocytes is greater than daily human exposure to A α C but comparable with the doses employed in studies investigating the genotoxicity of A α C (18, 19). The amount of A α C arising in mainstream smoke is 60–250 ng/cigarette (7, 8). Thus, the intracellular or plasma levels of A α C found in humans exposed to this tobacco carcinogen are considerably lower than the amount of A α C employed in our hepatocyte study. However, dG-C8-A α C formation occurs in a concentration-dependent

manner in human hepatocytes treated with A α C over a 10,000-fold concentration range (1 nM to 10 μ M), signifying that the reactive *N*-oxidation metabolites of A α C are formed at physiological exposure levels (20). More sensitive mass spectrometry-based methods are required for measuring A α C-albumin adducts and albumin oxidation products in hepatocytes at these lower exposure conditions to A α C.

The Cys³⁴ of albumin accounts for 80% of total free thiol content in plasma and is considered a major antioxidant and scavenger of electrophiles in plasma (34). A number of genotoxicants and toxic electrophiles form adducts with the Cys³⁴ of rodent or human albumin (23). Many of these adducts have been characterized primarily *in vitro*, and several adducts have been detected in humans. Albumin adducts have been identified with acrylamide (70), nitrogen mustard (71), α,β -unsaturated aldehydes (26), the neurotoxin brevetoxin B (72), acetaminophen (42), benzene (23), and several *N*-oxidized HAAs of diverse structures (32, 35, 56, 73). In addition, aldehydes produced in tobacco smoke are scavenged by Cys³⁴ of albumin *in vitro* (74). Immunochemical techniques have shown carbonyl residues are formed with albumin exposed to cigarette smoke extract, and the carbonylation of albumin, by tobacco smoke, has been detected in lung tissue biopsy samples of smokers (75). Spectrophotometric assays have shown a decrease in the free Cys³⁴ content of albumin following exposure to cigarette smoke extracts *in vitro* (74, 76). The diminution of free Cys³⁴ content may be attributed to adducts formed with aldehydes or by oxidation with ROS (26, 74, 77); however, a correlation between the level of adduct formation at Cys³⁴ of albumin and cigarette smoking constituents remains to be established *in vivo*. Recently, elevated levels of Cys³⁴-SO₂H of albumin were detected in plasma of smokers in a small pilot study (65). A α C, other HAAs, and structurally related aromatic amines present in tobacco smoke represent a class of chemicals in tobacco smoke that may contribute to the chemical modification or oxidation of Cys³⁴ and the oxidation of Met residues of albumin.

In summary, A α C, a rodent liver carcinogen (12), undergoes bioactivation and forms adducts with DNA and albumin and induces oxidative stress in human hepatocytes. Albumin is a potent scavenger of ROS species generated by A α C metabolites. A α C, other HAAs, and many aromatic amines that arise in mainstream tobacco smoke (1, 5, 66) undergo *N*-oxidation in humans (54). Some of these metabolites form adducts with DNA and protein and also induce oxidative stress, which may be contributing factors to liver damage and cancer risk in smokers. The Cys³⁴ adducts of *N*-oxidized HAAs and arylamines or their hydrolysis products and elevated levels of Cys³⁴-SO₂H and Cys³⁴-SO₃H of albumin may be potential biomarkers to assess exposure to these hazardous chemicals in tobacco smokers.

References

1. International Agency for Research on Cancer (1986) *IARC Monographs on the Evaluation of Carcinogenic Risks to Humans: Tobacco Smoking*, pp. 127–293, International Agency for Research on Cancer, Lyon, France
2. Lüchtenborg, M., White, K. K., Wilkens, L., Kolonel, L. N., and Le Marchand, L. (2007) Smoking and colorectal cancer: different effects by type of cigarettes? *Cancer Epidemiol. Biomarkers Prev.* **16**, 1341–1347
3. Giovannucci, E. (2001) An updated review of the epidemiological evidence that cigarette smoking increases risk of colorectal cancer. *Cancer Epide-*

- miol. Biomarkers Prev.* **10**, 725–731
4. Vineis, P., Alavanja, M., Buffler, P., Fontham, E., Franceschi, S., Gao, Y. T., Gupta, P. C., Hackshaw, A., Matos, E., Samet, J., Sitas, F., Smith, J., Stayner, L., Straif, K., Thun, M. J., Wichmann, H. E., Wu, A. H., Zaridze, D., Peto, R., and Doll, R. (2004) Tobacco and cancer: recent epidemiological evidence. *J. Natl. Cancer Inst.* **96**, 99–106
 5. Hoffmann, D., Hoffmann, I., and El-Bayoumy, K. (2001) The less harmful cigarette: a controversial issue: a tribute to Ernst L. Wynder. *Chem. Res. Toxicol.* **14**, 767–790
 6. Yoshida, D., Matsumoto, T., Yoshimura, R., and Matsuzaki, T. (1978) Mutagenicity of amino- α -carbolines in pyrolysis products of soybean globulin. *Biochem. Biophys. Res. Commun.* **83**, 915–920
 7. Yoshida, D., and Matsumoto, T. (1980) Amino- α -carbolines as mutagenic agents in cigarette smoke condensate. *Cancer Lett.* **10**, 141–149
 8. Zhang, L., Ashley, D. L., and Watson, C. H. (2011) Quantitative analysis of six heterocyclic aromatic amines in mainstream cigarette smoke condensate using isotope dilution liquid chromatography-electrospray ionization tandem mass spectrometry. *Nicotine Tob. Res.* **13**, 120–126
 9. International Agency for Research on Cancer (2002) *IARC Monographs on the Evaluation of Carcinogenic Risks to Humans: Tobacco Smoke and Involuntary Smoking*, pp. 1005–1403, International Agency for Research on Cancer, Lyon, France
 10. Kriek, E. (1992) Fifty years of research on *N*-acetyl-2-aminofluorene, one of the most versatile compounds in experimental cancer research. *J. Cancer Res. Clin. Oncol.* **118**, 481–489
 11. Turesky, R. J., Yuan, J. M., Wang, R., Peterson, S., and Yu, M. C. (2007) Tobacco smoking and urinary levels of 2-amino-9*H*-pyrido[2,3-*b*]indole in men of Shanghai, China. *Cancer Epidemiol. Biomarkers Prev.* **16**, 1554–1560
 12. Sugimura, T., Wakabayashi, K., Nakagama, H., and Nagao, M. (2004) Heterocyclic amines: Mutagens/carcinogens produced during cooking of meat and fish. *Cancer Sci.* **95**, 290–299
 13. Okonogi, H., Ushijima, T., Shimizu, H., Sugimura, T., and Nagao, M. (1997) Induction of aberrant crypt foci in C57BL/6N mice by 2-amino-9*H*-pyrido[2,3-*b*]indole (A α C) and 2-amino-3,8-dimethylimidazo[4,5-*f*]quinoxaline (MeIQx). *Cancer Lett.* **111**, 105–109
 14. Zhang, X. B., Felton, J. S., Tucker, J. D., Urlando, C., and Heddle, J. A. (1996) Intestinal mutagenicity of two carcinogenic food mutagens in transgenic mice: 2-amino-1-methyl-6-phenylimidazo[4,5-*b*]pyridine and amino(α)carboline. *Carcinogenesis* **17**, 2259–2265
 15. Niwa, T., Yamazoe, Y., and Kato, R. (1982) Metabolic activation of 2-amino-9*H*-pyrido[2,3-*b*]indole by rat-liver microsomes. *Mutat. Res.* **95**, 159–170
 16. Raza, H., King, R. S., Squires, R. B., Guengerich, F. P., Miller, D. W., Freeman, J. P., Lang, N. P., and Kadlubar, F. F. (1996) Metabolism of 2-amino- α -carboline: a food-borne heterocyclic amine mutagen and carcinogen by human and rodent liver microsomes and by human cytochrome P4501A2. *Drug Metab. Dispos.* **24**, 395–400
 17. King, R. S., Teitel, C. H., and Kadlubar, F. F. (2000) *In vitro* bioactivation of *N*-hydroxy-2-amino- α -carboline. *Carcinogenesis* **21**, 1347–1354
 18. Turesky, R. J., Bendaly, J., Yasa, I., Doll, M. A., and Hein, D. W. (2009) The impact of NAT2 acetylator genotype on mutagenesis and DNA adducts from 2-amino-9*H*-pyrido[2,3-*b*]indole. *Chem. Res. Toxicol.* **22**, 726–733
 19. Majer, B. J., Kassie, F., Sasaki, Y., Pfau, W., Glatt, H., Meinel, W., Darroudi, F., and Knasmüller, S. (2004) Investigation of the genotoxic effects of 2-amino-9*H*-pyrido[2,3-*b*]indole in different organs of rodents and in human derived cells. *J. Chromatogr. B Analyt. Technol. Biomed. Life Sci.* **802**, 167–173
 20. Nauwelaers, G., Bellamri, M., Fessard, V., Turesky, R. J., and Langouët, S. (2013) DNA adducts of the tobacco carcinogens 2-amino-9*H*-pyrido[2,3-*b*]indole and 4-aminobiphenyl are formed at environmental exposure levels and persist in human hepatocytes. *Chem. Res. Toxicol.* **26**, 1367–1377
 21. Miller, J. A. (1970) Carcinogenesis by chemicals: an overview: G. H. A. Clowes memorial lecture. *Cancer Res.* **30**, 559–576
 22. Törnqvist, M., Fred, C., Haglund, J., Helleberg, H., Paulsson, B., and Rydberg, P. (2002) Protein adducts: quantitative and qualitative aspects of their formation, analysis and applications. *J. Chromatogr. B Analyt. Technol. Biomed. Life Sci.* **778**, 279–308
 23. Rappaport, S. M., Li, H., Grigoryan, H., Funk, W. E., and Williams, E. R. (2012) Adductomics: characterizing exposures to reactive electrophiles. *Toxicol. Lett.* **213**, 83–90
 24. Liebler, D. C. (2002) Proteomic approaches to characterize protein modifications: new tools to study the effects of environmental exposures. *Environ. Health Perspect.* **110**, 3–9
 25. Rubino, F. M., Pitton, M., Di Fabio, D., and Colombi, A. (2009) Toward an “omic” physiopathology of reactive chemicals: thirty years of mass spectrometric study of the protein adducts with endogenous and xenobiotic compounds. *Mass Spectrom. Rev.* **28**, 725–784
 26. Aldini, G., Regazzoni, L., Orioli, M., Rimoldi, I., Facino, R. M., and Carini, M. (2008) A tandem MS precursor-ion scan approach to identify variable covalent modification of albumin Cys³⁴: a new tool for studying vascular carbonylation. *J. Mass Spectrom.* **43**, 1470–1481
 27. Skipper, P. L., and Tannenbaum, S. R. (1990) Protein adducts in the molecular dosimetry of chemical carcinogens. *Carcinogenesis* **11**, 507–518
 28. Yu, M. C., Skipper, P. L., Tannenbaum, S. R., Chan, K. K., and Ross, R. K. (2002) Arylamine exposures and bladder cancer risk. *Mutat. Res.* **506**, 21–28
 29. Peng, L., and Turesky, R. J. (2014) Optimizing proteolytic digestion conditions for the analysis of serum albumin adducts of 2-amino-1-methyl-6-phenylimidazo[4,5-*b*]pyridine, a potential human carcinogen formed in cooked meat. *J. Proteomics* **103**, 267–278
 30. Peng, L., and Turesky, R. J. (2013) Capturing labile sulfenamide and sulfenamide serum albumin adducts of carcinogenic arylamines by chemical oxidation. *Anal. Chem.* **85**, 1065–1072
 31. Westra, J. G. (1981) A rapid and simple synthesis of reactive metabolites of carcinogenic aromatic amines in high yield. *Carcinogenesis* **2**, 355–357
 32. Peng, L., and Turesky, R. J. (2011) Mass spectrometric characterization of 2-amino-1-methyl-6-phenylimidazo[4,5-*b*]pyridine *N*-oxidized metabolites bound at Cys³⁴ of human serum albumin. *Chem. Res. Toxicol.* **24**, 2004–2017
 33. Nauwelaers, G., Bessette, E. E., Gu, D., Tang, Y., Rageul, J., Fessard, V., Yuan, J. M., Yu, M. C., Langouët, S., and Turesky, R. J. (2011) DNA adduct formation of 4-aminobiphenyl and heterocyclic aromatic amines in human hepatocytes. *Chem. Res. Toxicol.* **24**, 913–925
 34. Carballal, S., Radi, R., Kirk, M. C., Barnes, S., Freeman, B. A., and Alvarez, B. (2003) Sulfenic acid formation in human serum albumin by hydrogen peroxide and peroxyntirite. *Biochemistry* **42**, 9906–9914
 35. Turesky, R. J., Skipper, P. L., and Tannenbaum, S. R. (1987) Binding of 2-amino-3-methylimidazo[4,5-*f*]quinoline to hemoglobin and albumin *in vivo* in the rat: identification of an adduct suitable for dosimetry. *Carcinogenesis* **8**, 1537–1542
 36. Turesky, R. J., and Markovic, J. (1994) DNA adduct formation of the food carcinogen 2-amino-3-methylimidazo[4,5-*f*]quinoline at the C-8 and N2 atoms of guanine. *Chem. Res. Toxicol.* **7**, 752–761
 37. Langouët, S., Coles, B., Morel, F., Becquemont, L., Beaune, P., Guengerich, F. P., Ketterer, B., and Guillouzo, A. (1995) Inhibition of CYP1A2 and CYP3A4 by oltipraz results in reduction of aflatoxin B1 metabolism in human hepatocytes in primary culture. *Cancer Res.* **55**, 5574–5579
 38. Tang, Y., Kassie, F., Qian, X., Ansha, B., and Turesky, R. J. (2013) DNA adduct formation of 2-amino-9*H*-pyrido[2,3-*b*]indole and 2-amino-3,4-dimethylimidazo[4,5-*f*]quinoline in mouse liver and extrahepatic tissues during a subchronic feeding study. *Toxicol. Sci.* **133**, 248–258
 39. Tabb, D. L., Fernando, C. G., and Chambers, M. C. (2007) MyriMatch: highly accurate tandem mass spectral peptide identification by multivariate hypergeometric analysis. *J. Proteome Res.* **6**, 654–661
 40. Goodenough, A. K., Schut, H. A., and Turesky, R. J. (2007) Novel LC-ESI/MS/MS *n* method for the characterization and quantification of 2'-deoxyguanosine adducts of the dietary carcinogen 2-amino-1-methyl-6-phenylimidazo[4,5-*b*]pyridine by 2-D linear quadrupole ion trap mass spectrometry. *Chem. Res. Toxicol.* **20**, 263–276
 41. Kang, P., Dalvie, D., Smith, E., Zhou, S., and Deese, A. (2007) Identification of a novel glutathione conjugate of flutamide in incubations with human liver microsomes. *Drug Metab. Dispos.* **35**, 1081–1088
 42. Damsten, M. C., Commandeur, J. N., Fidler, A., Hulst, A. G., Touw, D., Noort, D., and Vermeulen, N. P. (2007) Liquid chromatography/tandem mass spectrometry detection of covalent binding of acetaminophen to human serum albumin. *Drug Metab. Dispos.* **35**, 1408–1417
 43. Saito, K., and Kato, R. (1984) Glutathione conjugation of arylnitroso com-

Characterization of A α C-Serum Albumin Adducts

- pound: detection and monitoring labile intermediates *in situ* inside a fast atom bombardment mass spectrometer. *Biochem. Biophys. Res. Commun.* **124**, 1–5
44. Eyer, P., and Galleman, D. (1996) in *The Chemistry of Amine, Nitroso, Nitro and Related Groups*, Part 1 (Patai, S., ed) pp. 999–1040, John Wiley & Sons, Chichester, UK
 45. Lemke, T. L., Roche, V. F., and Zito, S. W. (2012) *Review of Organic Functional Groups: Introduction to Medicinal Organic Chemistry*, 5th Ed., pp. 85–87, Lippincott Williams & Wilkins, Baltimore, MD
 46. Novak, M., and Kazerani, S. (2000) Characterization of the 2-(α -carbonyl)nitrenium ion and its conjugate base produced during the decomposition of the model carcinogen 2-*N*-(pivaloyloxy)-2-amino- α -carboline in aqueous solution. *J. Am. Chem. Soc.* **122**, 3606–3616
 47. Steen, H., and Mann, M. (2001) Similarity between condensed phase and gas phase chemistry: fragmentation of peptides containing oxidized cysteine residues and its implications for proteomics. *J. Am. Soc. Mass Spectrom.* **12**, 228–232
 48. Novak, M., and Nguyen, T. M. (2003) Unusual reactions of the model carcinogen *N*-acetoxy-*N*-acetyl-2-amino- α -carboline. *J. Org. Chem.* **68**, 9875–9881
 49. Murata, M., and Kawanishi, S. (2011) Mechanisms of oxidative DNA damage induced by carcinogenic arylamines. *Front. Biosci. (Landmark Ed.)* **16**, 1132–1143
 50. Colombo, G., Clerici, M., Giustarini, D., Rossi, R., Milzani, A., and Dalle-Donne, I. (2012) Redox albuminomics: oxidized albumin in human diseases. *Antioxid. Redox Signal.* **17**, 1515–1527
 51. Finch, J. W., Crouch, R. K., Knapp, D. R., and Schey, K. L. (1993) Mass spectrometric identification of modifications to human serum albumin treated with hydrogen peroxide. *Arch. Biochem. Biophys.* **305**, 595–599
 52. Bruschi, M., Petretto, A., Candiano, G., Musante, L., Movilli, E., Santucci, L., Urbani, A., Gusmano, R., Verrina, E., Cancarini, G., Scolari, F., and Ghiggeri, G. M. (2008) Determination of the oxido-redox status of plasma albumin in hemodialysis patients. *J. Chromatogr. B Analyt. Technol. Biomed. Life Sci.* **864**, 29–37
 53. Guillouzo, A. (1998) Liver cell models in *in vitro* toxicology. *Environ. Health Perspect.* **106**, 511–532
 54. Turesky, R. J., and Le Marchand, L. (2011) Metabolism and biomarkers of heterocyclic aromatic amines in molecular epidemiology studies: lessons learned from aromatic amines. *Chem. Res. Toxicol.* **24**, 1169–1214
 55. Felton, J. S., Jagerstad, M., Knize, M. G., Skog, K., and Wakabayashi, K. (2000) in *Food Borne Carcinogens Heterocyclic Amines* (Nagao, M., and Sugimura, T., eds) pp. 31–71, John Wiley & Sons Ltd., Chichester, UK
 56. Peng, L., Dasari, S., Tabb, D. L., and Turesky, R. J. (2012) Mapping serum albumin adducts of the food-borne carcinogen 2-amino-1-methyl-6-phenylimidazo[4,5-*b*]pyridine by data-dependent tandem mass spectrometry. *Chem. Res. Toxicol.* **25**, 2179–2193
 57. John, H., Breyer, F., Thumfart, J. O., Höchstetter, H., and Thiermann, H. (2010) Matrix-assisted laser desorption/ionization time-of-flight mass spectrometry (MALDI-TOF MS) for detection and identification of albumin phosphorylation by organophosphorus pesticides and G- and V-type nerve agents. *Anal. Bioanal. Chem.* **398**, 2677–2691
 58. Noort, D., Hulst, A. G., van Zuylen, A., van Rijssel, E., and van der Schans, M. J. (2009) Covalent binding of organophosphorothioates to albumin: a new perspective for OP-pesticide biomonitoring? *Arch. Toxicol.* **83**, 1031–1036
 59. Li, B., Schopfer, L. M., Hinrichs, S. H., Masson, P., and Lockridge, O. (2007) Matrix-assisted laser desorption/ionization time-of-flight mass spectrometry assay for organophosphorus toxicants bound to human albumin at Tyr⁴¹¹. *Anal. Biochem.* **361**, 263–272
 60. Turesky, R. J., Rossi, S. C., Welti, D. H., Lay, J. O., Jr., and Kadlubar, F. F. (1992) Characterization of DNA adducts formed *in vitro* by reaction of *N*-hydroxy-2-amino-3-methylimidazo[4,5-*f*]quinoline and *N*-hydroxy-2-amino-3,8-dimethylimidazo[4,5-*f*]quinoxaline at the C-8 and N2 atoms of guanine. *Chem. Res. Toxicol.* **5**, 479–490
 61. Snyderwine, E. G., Roller, P. P., Adamson, R. H., Sato, S., and Thorgerisson, S. S. (1988) Reaction of the *N*-hydroxylamine and *N*-acetoxy derivatives of 2-amino-3-methylimidazo[4,5-*f*]quinoline with DNA. Synthesis and identification of *N*-(deoxyguanosin-8-yl)-IQ. *Carcinogenesis* **9**, 1061–1065
 62. Frederiksen, H., Frandsen, H., and Pfau, W. (2004) Syntheses of DNA-adducts of two heterocyclic amines, 2-amino-3-methyl-9*H*-pyrido[2,3-*b*]indole (MeAaC) and 2-amino-9*H*-pyrido[2,3-*b*]indole (AaC) and identification of DNA-adducts in organs from rats dosed with MeAaC. *Carcinogenesis* **25**, 1525–1533
 63. Bessette, E. E., Spivack, S. D., Goodenough, A. K., Wang, T., Pinto, S., Kadlubar, F. F., and Turesky, R. J. (2010) Identification of carcinogen DNA adducts in human saliva by linear quadrupole ion trap/multistage tandem mass spectrometry. *Chem. Res. Toxicol.* **23**, 1234–1244
 64. Kim, D., Kadlubar, F. F., Teitel, C. H., and Guengerich, F. P. (2004) Formation and reduction of aryl and heterocyclic nitroso compounds and significance in the flux of hydroxylamines. *Chem. Res. Toxicol.* **17**, 529–536
 65. Grigoryan, H., Li, H., Iavarone, A. T., Williams, E. R., and Rappaport, S. M. (2012) Cys³⁴ adducts of reactive oxygen species in human serum albumin. *Chem. Res. Toxicol.* **25**, 1633–1642
 66. Hecht, S. S. (2003) Tobacco carcinogens, their biomarkers and tobacco-induced cancer. *Nat. Rev. Cancer* **3**, 733–744
 67. Siraki, A. G., Chan, T. S., Galati, G., Teng, S., and O'Brien, P. J. (2002) *N*-Oxidation of aromatic amines by intracellular oxidases. *Drug Metab. Rev.* **34**, 549–564
 68. Neumann, H. G. (2007) Aromatic amines in experimental cancer research: tissue-specific effects, an old problem and new solutions. *Crit. Rev. Toxicol.* **37**, 211–236
 69. Tsuneoka, Y., Dalton, T. P., Miller, M. L., Clay, C. D., Shertzer, H. G., Talaska, G., Medvedovic, M., and Nebert, D. W. (2003) 4-aminobiphenyl-induced liver and urinary bladder DNA adduct formation in Cyp1a2(–/–) and Cyp1a2(+ / +) mice. *J. Natl. Cancer Inst.* **95**, 1227–1237
 70. Noort, D., Fidder, A., and Hulst, A. G. (2003) Modification of human serum albumin by acrylamide at cysteine-34: a basis for a rapid biomonitoring procedure. *Arch. Toxicol.* **77**, 543–545
 71. Noort, D., Fidder, A., Hulst, A. G., Woolfitt, A. R., Ash, D., and Barr, J. R. (2004) Retrospective detection of exposure to sulfur mustard: improvements on an assay for liquid chromatography-tandem mass spectrometry analysis of albumin-sulfur mustard adducts. *J. Anal. Toxicol.* **28**, 333–338
 72. Wang, Z., and Ramsdell, J. S. (2011) Analysis of interactions of breventoxin-B and human serum albumin by liquid chromatography/mass spectrometry. *Chem. Res. Toxicol.* **24**, 54–64
 73. Reistad, R., Frandsen, H., Grivas, S., and Alexander, J. (1994) *In vitro* formation and degradation of 2-amino-1-methyl-6-phenylimidazo[4,5-*b*]pyridine (PhIP) protein adducts. *Carcinogenesis* **15**, 2547–2552
 74. Colombo, G., Aldini, G., Orioli, M., Giustarini, D., Gornati, R., Rossi, R., Colombo, R., Carini, M., Milzani, A., and Dalle-Donne, I. (2010) Water-Soluble α,β -unsaturated aldehydes of cigarette smoke induce carbonylation of human serum albumin. *Antioxid. Redox Signal.* **12**, 349–364
 75. Hackett, T. L., Scarci, M., Zheng, L., Tan, W., Treasure, T., and Warner, J. A. (2010) Oxidative modification of albumin in the parenchymal lung tissue of current smokers with chronic obstructive pulmonary disease. *Respir. Res.* **11**, 180
 76. Colombo, G., Rossi, R., Gagliano, N., Portinaro, N., Clerici, M., Annibal, A., Giustarini, D., Colombo, R., Milzani, A., and Dalle-Donne, I. (2012) Red blood cells protect albumin from cigarette smoke-induced oxidation. *PLoS One* **7**, e29930
 77. Colzani, M., Aldini, G., and Carini, M. (2013) Mass spectrometric approaches for the identification and quantification of reactive carbonyl species protein adducts. *J. Proteomics* **92**, 28–50